Ore Geology Reviews 125 (2020) 103693

Contents lists available at ScienceDirect

Ore Geology Reviews

journal homepage: www.elsevier.com/locate/oregeorev

REE fractionation during crystallization and alteration of fergusonite-(Y) from Zr-REE-Nb-rich late- to post-magmatic products of the Keivy alkali granite complex, NW Russia

Dmitry Zozulya[a,*], Ray Macdonald[b,c], Bogusław Bagiński[b]

[a] Geological Institute, Kola Science Centre, 14 Fersman Str, 184209 Apatity, Russia
[b] Institute of Geochemistry, Mineralogy and Petrology, University of Warsaw, al. Żwirki i Wigury 93, 02-089 Warsaw, Poland
[c] Environment Centre, Lancaster University, Lancaster LA1 4YQ, UK

ARTICLE INFO

Keywords:
Fergusonite-(Y)
Alkali granite
Pegmatite
Quartzolite
Metasomatite
REE fractionation

ABSTRACT

The Keivy alkali granite complex, Kola Peninsula, NW Russia, contains numerous Zr-REE-Y-Nb occurrences and deposits, formed by a complex sequence of pegmatitic, hydrothermal and metasomatic processes. The rare-metal rich lithologies have abundant fergusonite-(Y) mineralization. > 90 EPMA analyses of fergusonite-(Y) from different occurrences are used to document REE behavior during crystallization and alteration of the mineral. Variations in Y/HREE ratio during growth of fergusonite-(Y) in a pegmatite are explained by a change of the fluorine content in the fluid. Loss of Y and HREE and addition of Ce during alteration are governed by two major processes: Ce accumulation in late derivatives and high F contents in the crystallization environment. The decreases of Ce and other REE in some occurrences resulted from a low F content. The extent of alteration possibly depends on the actinide content in fergusonite-(Y) and the resulting radiation damage. Positive Eu/Eu* anomalies in fergusonite-(Y) from a number of occurrences were due to external contributions of Eu into the fluid from country rocks after the breakdown of plagioclase. The specific REE distribution in fergusonite-(Y) indicates crystallization at low CO_2/H_2O and changing F activity. A F-rich fluid is suggested during fergusonite-(Y) formation in alkali granite pegmatite and quartzolite, and a low-F fluid is characteristic of minerals from a metasomatite and amazonite pegmatite located in country rocks of alkali granite massifs.

1. Introduction

Accessory minerals are of great value as monitors of both magmatic evolution and postmagmatic processes affecting the host rocks, including hydrothermal alteration and metamorphism. Particularly useful in such studies are the high field strength elements (HFSE) and the rare earth elements (REE), which show, *inter alia*, variable mineral-melt partition coefficients during fractional crystallization and different mineral-fluid partitioning during hydrothermal processes. Studies of compositional changes and alteration processes in the REE-Nb-Ta-Ti oxide fergusonite are of petrological interest because the mineral can be considered as a monitor for the evolution of their host rocks and in particular of low-T geochemical processes operative in them (Ruschel et al., 2010). Here we use textural and compositional data for fergusonite-(Y) to explore late- and post-magmatic processes in a series of Zr-REE-Y-Nb occurrences and deposits from the Keivy alkaline province and, in particular, to show how the distribution of the REE was controlled by different fluid compositions and behavior in the different occurrences (granite, pegmatite, quartzolite, metasomatic rock).

Fergusonite has the general formula ABO4, where the A site is occupied by REE, Th, U and Ca, and the B site mainly by Nb, Ta and Ti. Depending on the dominant element in the A site, fergusonite-(Y), fergusonite-(Ce) and fergusonite-(Nd) are distinguished. Two structures have been reported for the mineral: a scheelite-type tetragonal fergusonite (α-fergusonite, $I4_1/a$) which transforms on heating at 1000 °C to a monoclinic polymorph (β-fergusonite, $I2/c$) (see review by Tomašić et al., 2006). As fergusonite usually contains high actinide concentrations (up to several wt.%), it is often prone to irradiation-induced amorphization and alteration. As in other REE–Nb–Ta–Ti oxides (minerals of the aeschynite, euxenite, pyrochlore and samarskite groups), compositional alteration may include secondary hydration; the addition of Ca, Al, Si, Ba, Sr; exchange of heavy rare earth elements (HREE) and Y for light rare earth elements (LREE); and loss of A-site cations (Ercit, 2005).

* Corresponding author.
E-mail address: zozulya@geoksc.apatity.ru (D. Zozulya).

https://doi.org/10.1016/j.oregeorev.2020.103693
Received 29 March 2020; Received in revised form 19 July 2020; Accepted 21 July 2020
Available online 25 July 2020

As an accessory mineral, fergusonite-(Y) is common in rare metal granites (Ervanne, 2004; Ercit, 2005) and in nepheline syenites (Olivo and Williams-Jones, 1999). Extremely rare fergusonite (Ce) and fergusonite-(Nd) are related rather to carbonatites, e.g. Novopavlovka, Ukraine (Kapustin, 1976); Ilmeny and Vishnevy Mts (Levin et al., 1997), Biraya (Mills et al., 2012) in Russia; and Bayan Obo, China (Weilang, 1991). Formanite-(Y), the Ta-analogue of fergusonite-(Y), has been found in granite pegmatites, such as Ploskaya Mt, NW Russia (Voloshin et al., 2003); East Pilbara Shire, West Australia (Wylie, 1954); and the Lac-du-Bonnet area, Manitoba (Masau et al., 2002). Fergusonite-(Y) can be a locally important phase in pegmatites of the gadolinite type (REL-REE (rare-element – rare earth elements)) subclass and rare-element class) of NYF (niobium, yttrium, fluorine) family, according to the pegmatite classification of Černý and Ercit (2005). Occurrences of fergusonite-(Y) from the type localities of rare-element pegmatites are the Arendal pegmatite field in Norway (Brøgger, 1906; Barth, 1927; Nilssen, 1970); Haldzan Buragtag, Mongolian Altai (Macdonald et al., 2015); Ilmeny, South Ural, Russia (Kobyashev and Nikandrov, 2007); Kola Peninsula, Russia (Voloshin and Pakhomovskii, 1986); West Australia (Calderwood et al., 2007); Madagascar (Ruschel et al., 2010; Estrade et al., 2014); East Egypt (Sami et al., 2017; Abu Elatta, 2019); and the Alps, Italy (Gieré et al., 2009). Fergusonite may form different species in a single rare-element pegmatite body (e.g. fergusonite-(Y), fergusonite-(Ce) and fergusonite-(Nd) in the Tatyana pegmatite, Haldzan Buragtag alkali granite massif, Mongolian Altai (Macdonald et al., 2015; Bagiński et al., 2016), thus being a sensitive indicator of REE fractionation during the evolution of pegmatite. Fergusonite-(Y) can be regarded as a perspective source of Y and HREE from rare-metal granites and albitites with disseminated REE-Nb-U mineralization, such as the Salem deposit in Tamil Nadu, India (Nishimori et al., 1977; Roy and Dhana Raju, 1999) and the Aryskan deposit in the Sayany Mts, Russia (Grigoriev and Sergeeva, 1993).

2. Geological background and Zr-REE-Nb-rich occurrences related to Keivy alkali granite

The Keivy alkaline province consists of 2.67–2.65 Ga aegirine-arfvedsonite granites comprising six sheet-like massifs a few hundred meters thick and with a total exposure area of ca. 2500 km^2. The largest massifs are West Keivy (1200 km^2), Ponoj (700 km^2) and White Tundra (120 km^2). Aegirine-augite-annite-ferrohastingsite syenogranites occur at the margins of some massifs. Typical unaltered alkali granite is massive with a porphyritic structure, with large (1.5–2.0 cm) subhedral phenocrysts of microcline-perthite (40 vol%) and a fine- to medium-grained groundmass composed of equal amounts of xenomorphic albite, quartz, microcline, and shlieren-like segregations of arfvedsonite and aegirine (± aenigmatite, astrophyllite). The morphology of microcline-perthite phenocrysts and albite–oligoclase ingrowths therein, along with the lack of inclusions of late dark-colored minerals, allow us to refer to the microcline-perthite as a primary magmatic mineral. The alkali granite is a leucocratic variety; the amount of mafic minerals does not exceed 7–8 vol%. The rock is typical of the White Tundra massif but drastically differs from the West Keivy granite, which always shows gneissic structure (linear-planar distribution of mafic minerals) and a subsolvus character (K-feldspar and albite). The above-mentioned variations in the structure of granites from certain massifs in the Keivy province can be explained by different degrees of a late metamorphic overprint. The granites intrude the TTG basement of the Central Kola terrane (NE Fennoscandian shield) and acid-intermediate metavolcanics of the Lebyazha Formation of the Keivy complex (Fig. 1). Lepidomelane-ferrohastingsite syenite and lepidomelane-aegirine nepheline syenite dykes outcrop within the West Keivy massif. Voluminous coeval gabbro-anorthosites are spatially confined to the Keivy alkali granites.

The granites of the Keivy province are very enriched in Zr (300–3500 ppm, average 1100 ppm), Y (40–250 ppm, average 90 ppm), Nb (30–170 ppm, average 70 ppm), REE (100–1000 times chondrite), which has been explained by derivation from enriched mantle sources for the primary melts and protracted crystal fractionation (Zozulya et al., 2012). Their peralkaline and feroan character, and elevated HFSE contents suggest that the Keivy granites are A-type granitoids. To our knowledge this is the one of the earliest occurrences of A-granite magmatism on Earth (Mitrofanov et al., 2000). Numerous Zr-Y-REE-Nb ore occurrences and deposits are associated with different lithologies and were formed by various petrogenetic (late- and post-magmatic) processes (Fig. 1).

2.1. Mineralized granite

Mineralized (rare-metal) granite forms bodies up to 1.5 × 4 km in surface area located in the apical parts of alkali granite massifs (Fig. 1). The rocks are silica-rich (up to 40–50 vol% of quartz) and enriched in Zr (700–21,000 ppm, average 4700 ppm), Y (100–3900 ppm, average 550 ppm), Nb (40–400 ppm, average 180 ppm), REE (1000–1800 ppm, average 1300 ppm), Th (20–150 ppm), and U (5–23 ppm).

The main REE- and actinide-bearing minerals are chevkinite-(Ce), bastnäsite-(Ce), allanite-(Ce), fergusonite-(Y), monazite-(Ce), britholite-(Y), thorite, xenotime-(Y), REE-rich fluorapatite and pyrochlore-group minerals. The rare-metal minerals have certain features pointing to a hydrothermal origin, namely a chain-like distribution of porous and metamict zircon, bud-shaped aggregates of zircon, alteration rims on anhedral chevkinite and britholite, and the presence of REE-rich carbonate phases.

2.2. Pegmatite bodies

Dozens of pegmatite bodies from the Keivy province are confined to the inner and outer apical parts of alkali granite intrusions. They are a few tens of meters long and several meters wide, sometimes with schlieren and oval forms. Pegmatites are subdivided into quartz-microcline and quartz-feldspar-astrophyllite types. The most abundant rare-element minerals are zircon, fergusonite-(Y), gadolinite-(Y), and thorite. Keivy pegmatites are of NYF family and the gadolinite type, with an Y, HREE, Zr, Ti, Nb > Ta, F signature according to the classification of Ćerny and Ercit (2005). Undoubtedly A-type granites are the source of the Keivy pegmatites, which is confirmed by the same age of a pegmatitic zircon, 2656 Ma (Lyalina et al., 2012). Pegmatite from the White Tundra massif (Fig. 1, coordinates 67.49912:35.80254) has a quartz-rich core rimmed by a pegmatoidal aegirine-arfvedsonite granite. The body is elongated (2 × 5 m). In addition to common rare-metal mineralization (zircon, fergusonite-(Y), gadolinite-(Y), thorite, monazite, allanite-(Ce), kainosite-(Y), astrophyllite, britholite-group minerals), the pegmatite is characterized by abundant galena and secondary REE mineralization (tengerite-(Y), bastnäsite-(Y)). The fergusonite studied here is from two zones with different mineral assemblages; sample 2-4-4 is from the quartz zone with abundant secondary Y-REE mineralization, and sample 2-8-4 is from the quartz-feldspar zone enriched in zircon, titanite and astrophyllite.

A unique pegmatite body of amazonite-quartz-albite composition (Ploskaya Mt, coordinates 67.63333:36.70000) intrudes the Keivy metavolcanic complex. It is several hundred meters long and several tens of meters wide. Rare-element mineralization is represented by “plumbomicrolite”, betafite, columbite, plumbopyrochlore, keyviite-(Y), keyviite-(Yb), yttrofluorite, tveitite-(Y), xenotime-(Y), xenotime-(Yb), zircon, monazite-(Ce), gadolinite-(Y), hingganite-(Y), hingganite-(Yb), kuliokite-(Y), vyuntspakhite-(Y), kamphaugite-(Y), iimorite-(Y), bastnäsite-(Ce), tengerite-(Y), caysichite-(Y), thalenite-(Y), polylithionite, kainosite-(Y) and cassiterite and has a Y, Yb, Nb, Ta, F, P, Li, Be, Sn (Pb, W, Mo) geochemical signature, indicating the mixed NYF (Nb-Y-F) – LCT (Li-Cs-Ta) family. U-Pb ages ranging from 1673 to 1695 Ma have been obtained for xenotime, zircon and monazite from the pegmatite (Bayanova, 2004). No granite of the same age is known in

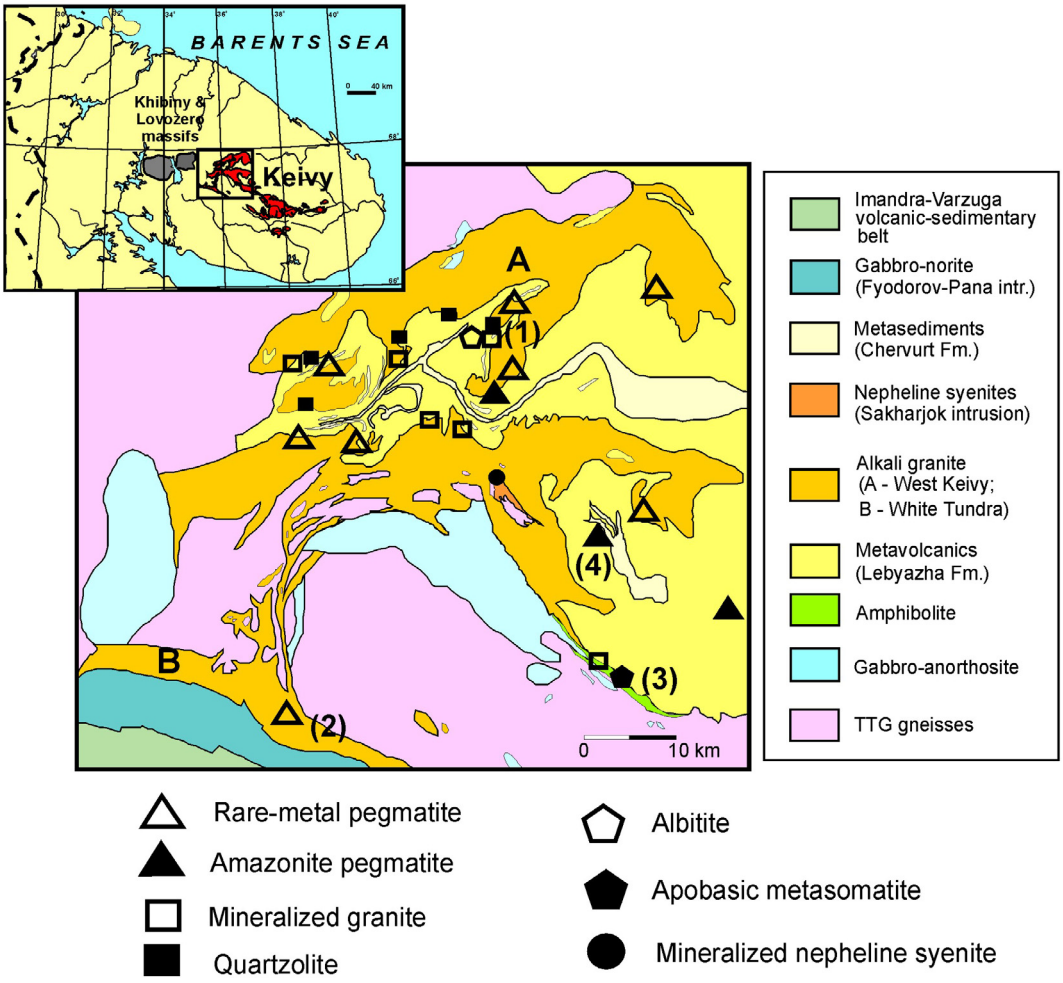

Fig. 1. Simplified geological map of the western part of the Keivy alkaline province, Kola Peninsula, NW Russia (modified after Batijeva (1976)), showing the location of Zr-REE-Y-Nb ore occurrences and deposits associated with different lithologies. Numbered occurrences are studied in this paper (1 – Rova quartzolite; 2 – White Tundra pegmatite; 3 – El'ozero quartz-epidote (apobasic) metasomatite; 4 – Ploskaya Mt amazonite pegmatite). The insert shows the location and structure of the Keivy alkali granite complex (boxed area).

Keivy and Kola and formation of the pegmatite by metamorphic remobilization of rare metals from an alkali granite and the host gneissic rock has been suggested (Zozulya et al., 2017). Voloshin and Pakhomovskii (1986) described two generations of fergusonite in the amazonite pegmatite: fergusonite-(Y) I and fergusonite-(Y) II. The first is confined mainly to the albitization zone of the pegmatite and is characterized by the formation of euhedral crystals and their replacement by plumbopyrochlore, columbite, xenotime and other minerals. The fergusonite-(Y) II occurs in cracks in previously crystallized tantaloniobates and also forms pseudomorphs after galena and plumbopyrochlore, and locally the latest thin intersecting veins. Fergusonite-(Y) I is always richer in uranium and thorium, and fergusonite-(Y) II is characterized by an absence of radioactive elements and higher contents of Ta and Yb. Formanite-(Y) is associated with fergusonite-(Y) II. The pegmatite is remarkable for its abundant and diverse Y- and HREE-minerals; the high content of volatile-rich minerals indicates a crucial role for F and CO_2 in pegmatite formation (Pekov et al., 2008).

2.3. Quartzolites

Quartzolites occur at the apical parts of alkali granite intrusions, where they are hosted by both the granites and the country rocks. The Rova occurrence (Fig. 1, sample 1–93, coordinates 67.85287:36.48994) is described here. Most quartzolite bodies from Rova vary from 0.5 to 1.5 m across. They are inequigranular, taxitic rocks, ranging from medium-grained to pegmatitic. A distinguishing feature is the very low content of alkali feldspars (K-feldspar and albite occur in different proportion and comprise < 10 vol%). Quartz contents range from 50 to 90 vol%. The primary mafic rock-forming mineral is aegirine or arfvedsonite; occasionally they are present in equal amounts. Magnetite and ilmenite also frequently occur as abundant minerals but also in smaller amounts. Sporadic large annite laths occur in some bodies. The significant amounts of fluorite and other F- and OH-bearing minerals point to the active involvement of fluids in the formation of the quartzolites. The whole rock may contain up to 30,000–40,000 ppm REE, 14,000 ppm Nb, 6.5 wt% ZrO_2, and 2.5 wt% Y_2O_3.

The rare-metal mineralization in the Keivy quartzolites is volumetrically significant (up to 20–30 vol%) and variable in composition. Zircon is the typical mineral of the ore assemblages. Other rare-metal minerals are irregularly distributed (from a few grams to tens of kilograms per ton of rock) and include aeschynite-(Y), chevkinite-(Ce), fergusonite-(Y), britholite-group minerals, yttrialite-(Y), thorite, monazite-(Ce), xenotime-(Y) and bastnäsite-(Ce). Fluorbritholite-(Y), yttrialite-(Y), fergusonite-(Y) and chevkinite-(Ce) are normally the main REE carriers and their overall content can reach 15–18 vol%. Fergusonite is common in some Rova quartzolite bodies, its content ranging from 5 to 10 vol%. The rare-metal minerals in quartzolite tend to form aggregates embedded in a quartz matrix. The minerals clearly are broadly coeval; mutual contacts between the phases are sharp and occasionally one phase forms inclusions in another, such as zircon in

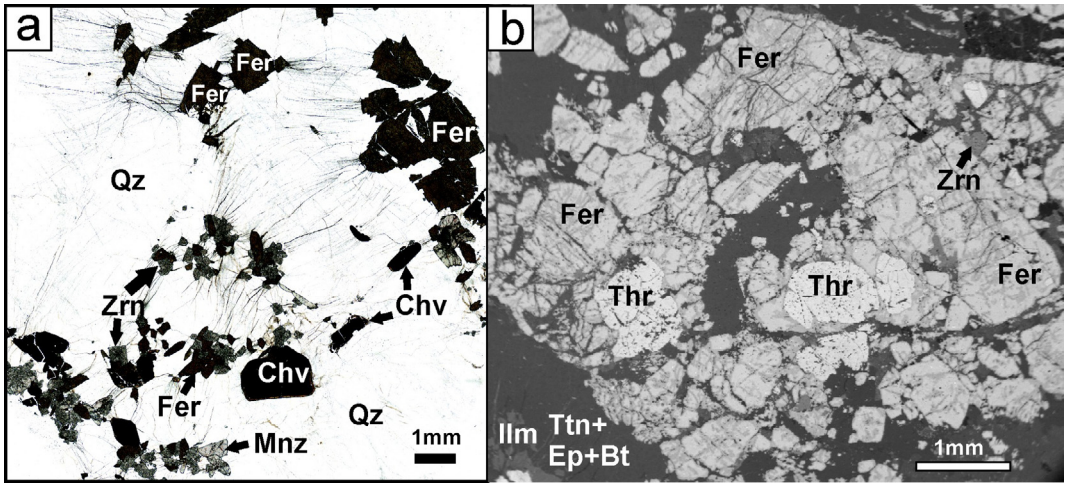

Fig. 2. Textural relationships of fergusonite-rich lithologies, related to the Keivy alkali granite (a) Rova quartzolite, sample 1–93 (plane polarized light); (b) El'ozero metasomatite, sample El-127 (BSE image). Fer – fergusonite-(Y), Chv – chevkinite-(Ce), Mnz – monazite, Thr – thorite, Zrn – zircon, Qz – quartz, Ilm – ilmenite. Ttn – titanite, Ep – epidote, Bt – biotite.

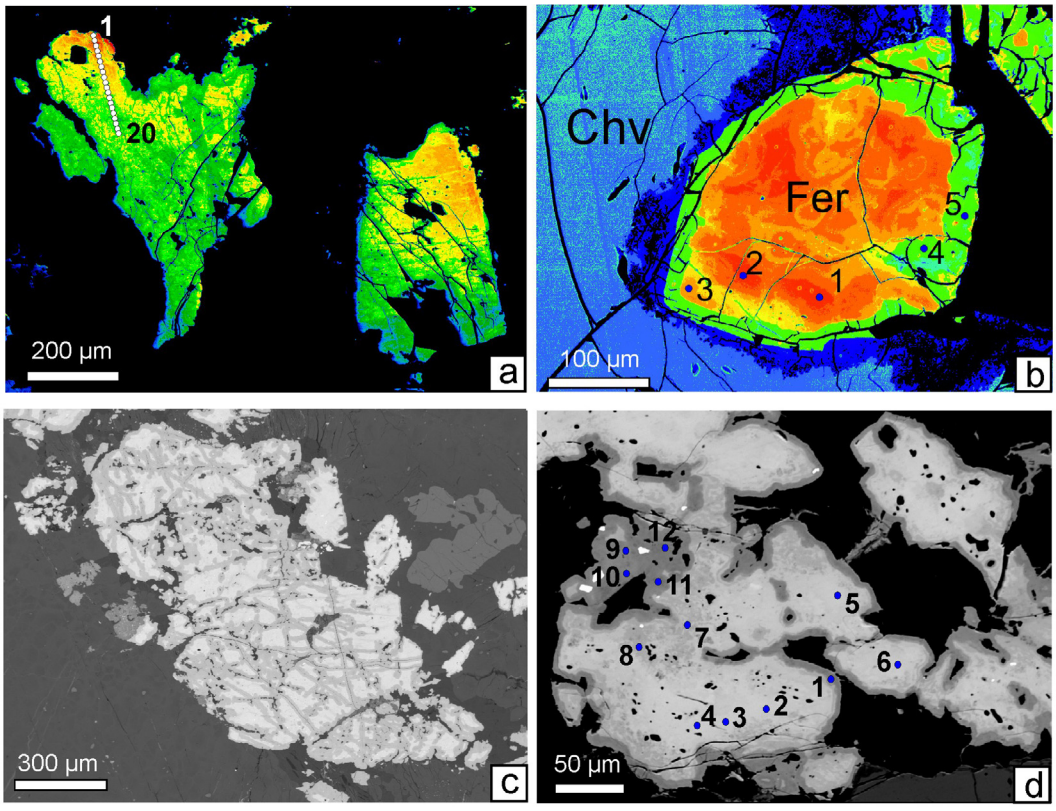

Fig. 3. Morphology and internal texture of Keivy fergusonite-(Y): (a) False colour BSE image of fergusonite-(Y) I from White Tundra pegmatite (1–20 – profile with 20 analyzed points); (b) False colour BSE image of fergusonite-(Y) from Rova quartzolite with analyzed points, note the alteration rim around chevkinite at the contact with fergusonite, possibly due to expansion of fergusonite during metamictization; (c) BSE image of fergusonite-(Y) from El'ozero metasomatite; (d) BSE image of fergusonite-(Y) II from White Tundra pegmatite with analyzed points. Mineral abbreviations as in Fig. 2. Analyses points are listed in Tables 1, 2, and in Supplementary Table S2. Figures (a) and (b): the range from blue/green through yellow to red corresponds to the increase of HREE/Y in mineral. (For interpretation of the references to colour in this figure legend, the reader is referred to the web version of this article.)

monazite and fergusonite in chevkinite (Fig. 2a). Expansion of fergusonite during metamictization may have caused the alteration rims around chevkinite at the contact with fergusonite (Fig. 3b) and cracks in host quartz (Fig. 2a).

2.4. Metasomatites

The metasomatic rocks studied here, from the El'ozero occurrence (Fig. 1, sample El-127, coordinates 67.49556:36.72639), are confined to a linear tectonic zone at the contact between the Keivy terrane and the Central Kola composite terrane. The zone strikes in a SE-NW direction for ca. 12 km and has an outcrop width varying from 200 to 1500 m. A few hundred alkali granite and aplite veins are confined to this zone and are concordant with the faults. The length of the veins is 50–500 m, with widths of 3–50 m. The granites intruded and metasomatically altered a variety of rocks in the Keivy complex, namely,

gabbro-anorthosites, gabbro-amphibolites and gneisses.

The metasomatic alteration of gabbro-anorthosite due to the intrusion of granite veins ranges from unaltered rocks to more intensively altered types as follows; massive gabbro-anorthosite – plagioamphibolite – amphibole-biotite metasomatite – mineralized garnet-biotite metasomatite – mineralized biotite-albite metasomatite with quartz – (epidotic metasomatite). Rare-metal mineralization is confined to small linear and lensoid bodies, nodules and pods 0.5–2 m in size. The rocks are characterized by extremely high REE (85,000 ppm), Y (42,000 ppm), Nb (62,000 ppm), Zr (67,000 ppm), Th (17,000 ppm), and U (7,700 ppm). Rare-metal mineralization is represented by thorite, chevkinite-(Ce), ferriallanite-(Ce) and allanite-(Ce), zircon, monazite, fergusonite-(Y), samarskite-(Y), aeschynite-(Y), pyrochlore, Nb-bearing titanite and rutile, ilmenite, magnetite, cassiterite, "mieite-(Y)", REE-carbonates, uraninite and gadolinite-group minerals. Fergusonite-(Y) from the El'ozero quartz-epidote metasomatite is abundant, often forming accumulations; its content locally reaches 15–20 vol%. It is assumed that rare-metal minerals crystallized under low-temperature conditions, as most include zircons considered to be hydrothermal from the presence of porous, numerous mineral inclusions and the high contents of Y, REE and Hf. The sequences of crystallization and the compositions of the rare-metal minerals indicate that the metasomatites formed under the influence of alkaline, F-bearing fluids with high activities of CO_2, Si, Ca and Al at various stages (Bagiński et al., 2016).

3. Analytical methods

The chemical compositions of fergusonite-(Y) were determined using electron microprobe analysis at the Inter-Institute Analytical Complex at the Institute of Geochemistry, Mineralogy, and Petrology, University of Warsaw, using a Cameca SX-100 microprobe equipped with four WDS detectors. The accelerating voltage was 15 kV and the probe current was 40nA. Counting times were 20 s on peak and 10 s on each of two background positions. The 'PAP' and 'X-PHI' φ(ρz) models (Pouchou and Pichoir, 1991; Merlet, 1994) were used for corrections.

The standards, crystals, and X-ray lines used and the detection limits are given in Supplementary Table S1. Representative electron microprobe data and mineral formulae for fergusonite-(Y) are given in Tables 1 and 2; the full data set for Keivy fergusonite (95 EPMA analyses, new and some published (Voloshin and Pakhomovskii, 1986; Bagiński et al., 2016; Macdonald et al., 2017)) is presented in Supplementary Table S2. Mineral formulae have been calculated on the basis of (Nb + Ta + Ti + W + Si) = 1 apfu, allocated to the *B* site of fergusonite. Two other possible formula calculations (on the basis of 2 cations (1) and of 4 oxygens (2)) are inappropriate due to regular overestimation of the *B* site cations (> 1) in case 1 and of the cation sum (> 2) in case 2.

4. Results

4.1. Morphology, textures, associated minerals and alteration

Fergusonites from the Keivy rare-metal occurrences usually form brown, heavily fractured crystals, varying from rectangular to prismatic, and rarely rounded (Fig. 2). They do not show interference colours under crossed polars, indicative of a high level of structural radiation damage, as noted by Ruschel et al. (2010) in fergusonite from the Berere region, Madagascar. XRD analysis was not undertaken during this study. An amorphous state for fergusonites from Keivy amazonite pegmatite and quartzolite has been reported (Voloshin and Pakhomovskii, 1986, and Bel'kov et al., 1988, respectively) and it is not unusual for a mineral of 2.65 Ga age. Nevertheless, we prefer the name "mineral" for the Keivy fergusonite. Expansion cracks have often formed radially around fergusonite grains. An important theme of this paper is the nature of the compositional alteration of the fergusonite. Such alteration is indicated by darker areas on BSE images, commonly giving a patchy appearance to grains, and by compositional criteria, particularly low analytical totals and non-stoichiometric formulae. In further discussion, we refer to unaltered and altered varieties.

Accessory fergusonite-(Y) from the *mineralized granites* usually occurs as small (up to 30 μm) rounded grains included in quartz, zircon and chevkinite-(Ce); rarely it forms chains of oval grains (up to 500 μm long) rimmed by annite along grain boundaries of quartz, microcline-perthite, magnetite and zircon (Mikhailova et al., 2017).

Fergusonite-(Y) from the Rova *quartzolite bodies* occurs as elongated spindle-like grains up to 10–12 mm in size; sometimes sheaf-shaped intergrowths of crystals are present. Fergusonite-(Y) is commonly included in quartz (Fig. 2a) and associated with fluorbritholite-(Y), growing along its boundaries. Rarely, the mineral is included in chevkinite (Fig. 3b), forming subhedral plates. It has a patchy, brighter core (orange on Fig. 3b), rimmed by a darker material (green) of variable thickness containing small areas of the brighter component. A notable feature of this sample is the expansion cracks radiating from the fergusonite crystals (Fig. 2a). The darker rims on the fergusonite-(Y) are clear textural evidence of late alteration.

Fergusonite-(Y) from the El'ozero *quartz-epidote metasomatite* forms large (> 1 cm) anhedral crystals, associated with thorite and zircon (included in fergusonite), set in an epidote-titanite-quartz-biotite matrix. The mineral has a network of fractures and patchy areas containing a darker component (Fig. 2b and 3c). It also forms residual "islands" enclosed in allanite-(Ce) (Bagiński et al., 2016). Among other REE–Nb–Ta–Ti oxides found in the metasomatite are accessory aeschynite-(Ce) and pyrochlore.

There are two morphological and apparently genetic types of accessory fergusonite in the *White Tundra pegmatite* depending on its location in the different zones of the pegmatite. The first (I) is present as euhedral/subhedral and angular crystals of 0.5–1 mm size in an aggregate of allanite, apatite, monazite and astrophyllite in a quartz matrix. No mineral inclusions have been found. This fergusonite shows a remarkable continuous zoning from high intensity BSE on one side of the crystals to lower intensity BSE on the opposite side (Fig. 3a). Fergusonite of the second type II forms large (up to 1–2 mm) intergrowths of numerous up to 100 μm, anhedral grains in a quartz-feldspar matrix (Fig. 3d). The mineral is characterized by the presence of inclusions of quartz and monazite and by alteration rims. The latter are clearly visible on BSE images due to their low intensity. The darker patches also occur in inner parts of the mineral.

4.2. Chemical composition and alteration trends

On the basis of internal textures and lithological occurrence four groups of Keivy fergusonites are distinguished in the compositional data set: fergusonite-(Y) I and fergusonite-(Y) II from the White Tundra pegmatite (WTP); fergusonite-(Y) from Rova quartzolie (RQ); and fergusonite-(Y) from the El'ozero metasomatite (EM) (Tables 1 and 2). In addition, representative published analyses of fergusonite from the Ploskaya amazonite pegmatite (PAP) (Voloshin and Pakhomovskii, 1986) are included. With the exception of fergusonite-(Y) I from the White Tundra pegmatite, all other groups of fergusonite show evidence of late alteration (rims and patches with lower BSE intensity). Most compositions fall into the fergusonite field of the classification scheme for REE–Nb–Ta–Ti oxides of Ercit (2005), with the exception of single minerals from WTP and PAP, which lie in the samarskite field (Fig. 4a).

Unaltered fergusonite-(Y) from all groups has a dominance of Y (0.46–0.78 apfu) in the *A* site, with significant amounts of REE (0.22–0.46 apfu, with the exception of El'ozero (0.14–0.24 apfu)). Calcium is lowest in fergusonite-(Y) I from WTP (0.01–0.04 apfu), while in other groups it is more elevated (0.03–0.1 apfu in fergusonite-(Y) II from White Tundra; 0.04–0.09 apfu in RQ; 0.05–0.17 apfu in EM; 0.06–0.13 in PAP). Actinides and Fe have almost similar distributions between the groups as Ca. Uranium is ≤ 0.01 apfu in fergusonite-(Y) I from WTP, 0.015–0.02 apfu in fergusonite-(Y) II from WTP, 0.03–0.04

Table 1
Representative compositions of fergusonite-(Y) I from White Tundra pegmatite along the profile 1–20 (sample 2-4-4).

Analysis no wt.%	1	2	3	5	6	8	9	10	12	14	15	16	18	20
WO_3	0.18	0.23	0.33	0.51	0.28	0.57	0.58	0.62	0.53	0.85	0.75	0.67	0.68	0.43
Nb_2O_5	45.18	44.43	45.80	45.53	45.44	42.88	44.27	44.20	45.11	43.91	41.31	44.70	44.05	45.55
Ta_2O_5	0.21	0.21	0.30	0.30	0.29	0.72	0.75	0.67	1.24	0.85	0.90	0.67	0.83	1.08
SiO_2	0.05	0.09	0.09	0.26	0.03	1.28	0.69	0.61	0.15	0.62	2.60	0.43	1.04	0.13
TiO_2	0.50	0.74	0.56	0.57	0.57	0.61	0.65	0.69	0.70	0.89	0.75	0.76	0.77	0.55
ThO_2	0.79	0.80	0.88	0.72	0.84	1.05	0.92	0.95	0.86	1.16	1.95	1.22	1.18	0.70
UO_2	0.55	0.67	0.53	0.49	0.44	0.69	0.62	0.58	0.86	0.73	0.66	0.56	0.73	0.63
Y_2O_3	21.94	22.41	24.41	26.22	24.82	26.30	26.42	26.14	27.57	26.81	26.12	26.63	26.65	27.28
La_2O_3	bd	bd	bd	bd	0.06	0.15	bd	bd	bd	0.08	0.22	bd	0.11	bd
Ce_2O_3	bd	bd	bd	0.09	0.15	0.49	0.21	0.23	0.17	0.23	1.08	0.16	0.31	0.15
Pr_2O_3	bd	bd	bd	bd	bd	bd	0.23	bd	bd	bd	bd	bd	bd	bd
Nd_2O_3	0.28	0.21	bd	0.26	0.60	1.06	0.75	0.97	1.05	1.00	1.69	0.91	1.10	1.03
Sm_2O_3	bd	bd	bd	bd	bd	0.35	bd	0.36	0.46	0.41	0.50	0.13	0.42	0.49
Gd_2O_3	5.96	5.53	5.05	4.86	5.17	4.45	4.09	4.17	3.90	3.91	4.05	4.34	4.01	4.20
Tb_2O_3	1.19	1.26	1.02	0.97	1.03	0.83	0.73	0.75	0.56	0.62	0.69	0.63	0.62	0.64
Dy_2O_3	10.97	10.27	8.80	8.51	9.39	7.42	6.66	6.82	5.90	6.37	6.09	7.04	6.49	6.28
Ho_2O_3	1.26	1.24	0.99	1.02	1.13	0.93	0.70	0.71	0.71	0.72	0.70	0.75	0.77	0.74
Er_2O_3	5.95	5.95	5.56	5.11	5.19	5.01	5.11	5.25	4.73	4.92	4.65	4.99	4.95	4.82
Tm_2O_3	0.77	0.80	0.79	0.67	0.72	0.74	0.81	0.77	0.81	0.78	0.76	0.83	0.78	0.78
Yb_2O_3	2.73	2.93	3.04	2.51	2.32	2.98	3.28	3.26	3.04	3.02	2.98	2.94	2.99	3.26
Lu_2O_3	0.92	1.13	1.03	0.84	0.83	0.72	0.82	0.91	0.80	0.77	0.84	0.85	0.71	0.63
CaO	0.60	0.54	0.52	0.51	0.40	0.53	0.56	0.53	0.29	0.40	0.38	0.30	0.39	0.18
MnO	bd	0.08	bd	bd	bd	bd	bd	bd	bd	bd	bd	bd	bd	bd
PbO	bd	0.22	bd	bd	bd	bd	0.23	0.20	bd	bd	bd	bd	bd	bd
Na_2O	0.12	0.11	0.13	0.11	0.10	0.15	0.15	0.12	0.11	0.16	0.22	0.11	0.15	0.09
Total	100.52	99.97	100.14	100.13	99.91	100.18	99.32	99.68	99.67	99.47	100.23	99.87	100.10	99.96
Mineral formulae on the basis of (Nb + Ta + Ti + W + Si) = 1 per formula unit (apfu)														
Ca	0.031	0.028	0.026	0.025	0.020	0.027	0.028	0.027	0.014	0.020	0.018	0.015	0.019	0.009
Na	0.011	0.010	0.012	0.010	0.009	0.013	0.013	0.011	0.010	0.014	0.019	0.010	0.013	0.008
La	0.000	0.000	0.000	0.000	0.001	0.003	0.000	0.000	0.000	0.001	0.004	0.000	0.002	0.000
Ce	0.000	0.000	0.000	0.001	0.003	0.008	0.004	0.004	0.003	0.004	0.018	0.003	0.005	0.002
Pr	0.000	0.000	0.000	0.000	0.000	0.000	0.004	0.000	0.000	0.000	0.000	0.000	0.000	0.000
Nd	0.005	0.004	0.003	0.004	0.010	0.018	0.012	0.016	0.017	0.017	0.027	0.015	0.018	0.017
Sm	0.000	0.000	0.000	0.000	0.001	0.006	0.000	0.006	0.007	0.007	0.008	0.002	0.007	0.008
Gd	0.094	0.088	0.078	0.075	0.081	0.069	0.063	0.064	0.060	0.060	0.060	0.067	0.061	0.065
Tb	0.019	0.020	0.016	0.015	0.016	0.013	0.011	0.012	0.009	0.009	0.010	0.010	0.009	0.010
Dy	0.169	0.159	0.133	0.128	0.143	0.111	0.100	0.102	0.088	0.095	0.088	0.105	0.095	0.094
Ho	0.019	0.019	0.015	0.015	0.017	0.014	0.010	0.011	0.010	0.011	0.010	0.011	0.011	0.011
Er	0.089	0.090	0.082	0.075	0.077	0.073	0.074	0.077	0.069	0.072	0.066	0.073	0.071	0.070
Tm	0.011	0.012	0.012	0.010	0.011	0.011	0.012	0.011	0.012	0.011	0.011	0.012	0.011	0.011
Yb	0.040	0.043	0.043	0.036	0.033	0.042	0.046	0.046	0.043	0.043	0.041	0.042	0.042	0.046
Lu	0.013	0.016	0.015	0.012	0.012	0.010	0.011	0.013	0.011	0.011	0.011	0.012	0.010	0.009
Y	0.557	0.572	0.607	0.649	0.624	0.652	0.653	0.648	0.681	0.661	0.624	0.657	0.646	0.674
Pb	0.000	0.003	0.000	0.000	0.000	0.000	0.003	0.003	0.000	0.000	0.000	0.000	0.000	0.000
Th	0.009	0.009	0.009	0.008	0.009	0.011	0.010	0.010	0.009	0.012	0.020	0.013	0.012	0.007
U	0.006	0.007	0.006	0.005	0.005	0.007	0.006	0.006	0.009	0.008	0.007	0.006	0.007	0.007
Mn	0.000	0.003	0.000	0.000	0.000	0.000	0.000	0.000	0.000	0.000	0.000	0.000	0.000	0.000
A cations	1.071	1.081	1.055	1.066	1.071	1.086	1.060	1.068	1.053	1.055	1.042	1.051	1.040	1.049
W	0.002	0.003	0.004	0.006	0.003	0.007	0.007	0.007	0.006	0.010	0.009	0.008	0.008	0.005
Nb	0.975	0.963	0.968	0.958	0.971	0.903	0.929	0.931	0.947	0.920	0.839	0.937	0.908	0.956
Ta	0.003	0.003	0.004	0.004	0.004	0.009	0.010	0.009	0.016	0.011	0.011	0.008	0.010	0.014
Ti	0.018	0.027	0.020	0.020	0.020	0.022	0.023	0.024	0.025	0.031	0.025	0.027	0.027	0.019
Si	0.002	0.004	0.004	0.012	0.001	0.060	0.032	0.028	0.007	0.029	0.117	0.020	0.047	0.006
B cations	1.000	1.000	1.000	1.000	1.000	1.000	1.000	1.000	1.000	1.000	1.000	1.000	1.000	1.000
Σ cations	2.071	2.081	2.055	2.066	2.071	2.086	2.060	2.068	2.053	2.055	2.042	2.051	2.040	2.049

Note. Al, Fe, Sn, Eu, Ba are below detection limit. bd – below detection limit.

apfu in RQ and EM, 0.01 in PAP. Thorium values are 0.01–0.02 apfu in fergusonite-(Y) I from WTP, but ≤ 0.01 apfu in fergusonite-(Y) II from WTP, 0.02–0.03 apfu in RQ, 0.01–0.03 apfu in EM, and 0.03 in PAP. No Fe was found in fergusonite-(Y) I from WTP, while in fergusonite-(Y) II from WTP it is 0.04–0.6 apfu, 0.01–0.04 apfu in RQ, and 0–0.02 in EM. The content of Pb is usually 0–0.01 apfu, with the exception of EM where it reaches 0.02 apfu.

Nb dominates the *B* site (0.84–0.98 apfu) in unaltered fergusonite, with low levels of Ta (< 0.01 apfu, with the exception of EM and PAP fergusonite-(Y) (0.03 and 0.045 apfu, respectively)). The *B* site also contains minor amounts of Ti (0.02–0.03 apfu in WTP fergusonite-(Y) I and II, 0.06–0.07 apfu in RQ, 0.01–0.05 apfu in EM, and 0.03 in PAP).

Altered fergusonite-(Y) shows steady increases in Ca (up to 0.19 apfu), Fe (up to 0.22 apfu), and Si (up to 0.26 apfu) contents and decreases in Y (0.66–0.32 apfu) and Nb (0.87–0.66 apfu). In some cases altered fergusonites-(Y) show elevated W and Pb (up 0.01 apfu) contents relative to its unaltered host. EM altered fergusonites-(Y) also have increased values of Al (up to 0.02 apfu). The sum of *A* cations behaves differently; it decreases to 0.97–0.80 apfu in WTP and RQ fergusonite-(Y) and increases to 1.06–1.318 apfu in EM fergusonite-(Y). The analytical totals may decrease to 91 wt%, inferring incorporation of significant amounts of O and OH into the mineral. We have not been able to identify a charge-balanced substitution scheme for compositional variations in the phase. Bagiński et al. (2016), using charge

Table 2
Representative compositions of fergusonite-(Y) from White Tundra pegmatite (fergusonite-(Y) II, sample 2–8-4), Rova quartzolite (sample 1–93) and El'ozero metasomatite (sample El-127).

Sample	2–8-4						1–93					El-127				
Analysis no	2	3	4	8 alt	9 alt	10 alt	1	2	3	4 alt	5 alt	3	4 alt	5 alt	9	10 alt
wt.%																
WO_3	bd	bd	bd	0.97	0.34	0.54	0.22	0.17	0.13	0.09	0.53	bd	0.25	0.35	0.17	0.47
Nb_2O_5	46.39	46.76	46.47	41.36	42.11	41.35	43.99	43.48	43.23	38.78	38.61	47.56	40.15	38.64	44.15	39.87
Ta_2O_5	0.46	0.52	0.42	1.56	0.97	0.76	0.45	0.41	0.47	0.49	0.55	2.03	2.45	2.29	2.03	2.13
SiO_2	0.27	bd	bd	7.99	4.30	5.03	0.09	0.18	1.43	5.74	6.71	0.05	1.22	1.98	0.30	4.23
TiO_2	0.81	0.78	0.71	1.34	1.60	0.87	1.72	1.70	1.73	1.62	1.57	0.36	0.29	0.28	0.77	0.46
SnO_2	bd	bd	bd	0.47	1.38	1.56	na	na	na	na	na	bd	bd	bd	bd	bd
ThO_2	0.60	0.55	0.45	0.74	0.58	0.71	2.24	2.70	2.20	1.88	1.92	1.31	1.16	1.12	2.44	2.10
UO_2	1.74	1.43	1.56	1.88	1.79	1.95	3.54	3.56	3.55	3.10	2.95	2.90	2.58	2.49	2.80	2.51
Al_2O_3	bd	bd	bd	bd	bd	bd	bd	bd	bd	0.02	bd	bd	0.13	0.42	bd	0.32
Y_2O_3	25.84	26.02	26.14	19.04	17.40	20.07	20.82	20.10	19.87	19.76	18.90	27.81	25.79	25.28	26.01	25.88
La_2O_3	bd	bd	bd	0.44	0.50	0.58	0.16	0.11	0.23	0.27	0.58	bd	0.08	0.09	bd	0.12
Ce_2O_3	0.26	0.18	0.15	0.76	1.21	1.17	0.70	0.76	0.71	0.77	1.58	bd	0.21	0.12	0.33	0.26
Pr_2O_3	bd	bd	bd	bd	bd	0.29	0.33	0.39	0.32	bd	0.38	bd	bd	bd	bd	bd
Nd_2O_3	0.67	0.62	0.70	0.82	1.11	1.12	2.28	2.26	2.01	1.87	1.97	0.48	0.28	0.32	1.12	0.50
Sm_2O_3	0.19	0.28	0.20	0.13	0.42	0.32	1.80	1.71	1.56	0.94	1.41	0.57	0.41	0.45	0.92	0.83
Eu_2O_3	bd	bd	bd	bd	bd	bd	1.36	1.19	1.41	1.29	1.09	bd	0.33	0.62	0.85	0.62
Gd_2O_3	0.49	0.47	0.55	0.73	0.89	0.88	3.58	3.46	3.48	3.13	3.24	1.40	1.07	1.22	1.53	1.30
Tb_2O_3	bd	bd	bd	bd	bd	bd	0.61	0.60	0.62	0.64	0.65	0.53	0.28	0.38	0.35	0.27
Dy_2O_3	1.99	2.37	2.34	2.32	2.16	2.29	5.22	5.15	4.86	4.63	4.30	3.24	2.76	2.81	2.88	2.68
Ho_2O_3	bd	bd	bd	0.21	0.16	bd	1.24	1.26	1.14	1.13	1.25	0.66	0.62	0.82	0.88	1.01
Er_2O_3	4.19	4.40	4.41	2.48	3.34	3.17	3.45	3.32	3.31	3.16	3.22	3.22	2.76	2.81	2.98	2.84
Tm_2O_3	0.80	0.81	0.85	0.49	0.67	0.61	0.45	0.32	0.49	bd	bd	na	na	na	na	na
Yb_2O_3	5.53	4.91	4.88	3.46	3.68	3.81	1.49	1.36	1.35	1.39	1.36	2.82	2.33	2.15	2.17	2.08
Lu_2O_3	1.04	1.02	0.83	0.60	0.74	0.68	0.35	0.62	0.48	1.13	0.58	0.43	0.40	0.55	bd	0.38
CaO	0.88	0.60	0.61	3.09	3.95	2.88	1.22	1.47	1.89	2.08	2.34	0.94	2.82	2.81	2.50	3.53
MnO	0.29	0.28	0.38	0.31	0.32	0.25	bd	0.11	0.08	0.12	bd	bd	0.31	0.29	0.07	0.12
FeO*	1.38	1.35	1.51	1.94	3.34	1.93	0.90	0.89	1.01	1.51	1.47	0.05	4.67	5.48	0.28	0.78
PbO	0.63	0.47	0.44	0.17	bd	bd	bd	bd	bd	0.52	bd	0.20	bd	bd	bd	0.35
Na_2O	0.05	0.04	0.06	0.10	0.06	0.05	na	na	na	na	na	0.06	bd	bd	bd	bd
Total	94.49	93.86	93.68	93.36	93.00	92.83	98.21	97.28	97.56	96.06	97.16	96.62	93.35	93.79	95.53	95.64
Mineral formulae on the basis of (Nb + Ta + Ti + W + Si) = 1 per formula unit (apfu)																
Ca	0.043	0.029	0.030	0.117	0.170	0.125	0.061	0.074	0.090	0.090	0.098	0.045	0.149	0.148	0.125	0.162
Na	0.004	0.004	0.006	0.007	0.005	0.004	0.000	0.000	0.000	0.000	0.000	0.005	0.000	0.002	0.000	0.000
La	0.000	0.000	0.000	0.006	0.007	0.009	0.003	0.002	0.004	0.004	0.008	0.000	0.001	0.002	0.000	0.002
Ce	0.004	0.003	0.002	0.010	0.018	0.017	0.012	0.013	0.012	0.011	0.023	0.000	0.004	0.002	0.006	0.004
Pr	0.000	0.000	0.000	0.000	0.000	0.004	0.006	0.007	0.005	0.000	0.005	0.000	0.000	0.000	0.000	0.000
Nd	0.011	0.010	0.012	0.010	0.016	0.016	0.038	0.038	0.032	0.027	0.027	0.008	0.005	0.006	0.019	0.008
Sm	0.003	0.004	0.003	0.002	0.006	0.004	0.029	0.028	0.024	0.013	0.019	0.009	0.007	0.008	0.015	0.012
Eu	0.000	0.000	0.000	0.000	0.000	0.000	0.022	0.019	0.021	0.018	0.015	0.000	0.006	0.010	0.014	0.009
Gd	0.007	0.007	0.008	0.009	0.012	0.012	0.055	0.054	0.051	0.042	0.042	0.021	0.017	0.020	0.024	0.018
Tb	0.000	0.000	0.000	0.000	0.000	0.000	0.009	0.009	0.009	0.009	0.008	0.008	0.005	0.006	0.005	0.004
Dy	0.029	0.035	0.035	0.026	0.028	0.030	0.078	0.078	0.070	0.061	0.054	0.047	0.044	0.044	0.043	0.037
Ho	0.000	0.000	0.000	0.002	0.002	0.000	0.018	0.019	0.016	0.015	0.016	0.009	0.010	0.013	0.013	0.014
Er	0.060	0.063	0.064	0.027	0.042	0.040	0.051	0.049	0.046	0.040	0.039	0.045	0.043	0.043	0.044	0.038
Tm	0.011	0.012	0.012	0.005	0.008	0.008	0.007	0.005	0.007	0.000	0.000	0.000	0.000	0.000	0.000	0.000
Yb	0.077	0.068	0.069	0.037	0.045	0.047	0.021	0.019	0.018	0.017	0.016	0.038	0.035	0.032	0.031	0.027
Lu	0.014	0.014	0.012	0.006	0.009	0.008	0.005	0.009	0.006	0.014	0.007	0.006	0.006	0.008	0.000	0.005
Y	0.626	0.633	0.642	0.357	0.372	0.432	0.517	0.503	0.471	0.427	0.392	0.661	0.675	0.660	0.646	0.591
Pb	0.008	0.006	0.005	0.002	0.000	0.001	0.000	0.000	0.000	0.006	0.000	0.002	0.000	0.000	0.000	0.004
Th	0.006	0.006	0.005	0.006	0.005	0.006	0.024	0.029	0.022	0.017	0.017	0.013	0.013	0.013	0.026	0.021
U	0.018	0.015	0.016	0.015	0.016	0.018	0.037	0.037	0.035	0.028	0.026	0.029	0.028	0.027	0.029	0.024
Fe**	0.052	0.052	0.058	0.057	0.112	0.065	0.035	0.035	0.038	0.051	0.048	0.002	0.192	0.225	0.011	0.028
Sn	0.000	0.000	0.000	0.007	0.022	0.025	0.000	0.000	0.000	0.000	0.000	0.000	0.000	0.000	0.000	0.000
Mn	0.011	0.011	0.015	0.009	0.011	0.008	0.000	0.004	0.003	0.004	0.000	0.000	0.013	0.012	0.003	0.004
Al	0.000	0.000	0.000	0.000	0.000	0.000	0.000	0.000	0.000	0.001	0.000	0.000	0.008	0.024	0.000	0.016
A cations	0.985	0.972	0.995	0.716	0.906	0.880	1.026	1.031	0.982	0.895	0.860	0.949	1.260	1.305	1.052	1.029
W	0.000	0.000	0.000	0.009	0.004	0.006	0.003	0.002	0.002	0.001	0.005	0.000	0.003	0.004	0.002	0.005
Nb	0.954	0.967	0.970	0.659	0.765	0.756	0.927	0.924	0.871	0.711	0.681	0.961	0.893	0.857	0.931	0.774
Ta	0.006	0.006	0.005	0.015	0.011	0.008	0.006	0.005	0.006	0.005	0.006	0.025	0.033	0.031	0.026	0.025
Ti	0.028	0.027	0.025	0.036	0.048	0.026	0.060	0.060	0.058	0.049	0.046	0.012	0.011	0.010	0.027	0.015
Si	0.012	0.000	0.000	0.282	0.173	0.203	0.004	0.008	0.064	0.233	0.262	0.002	0.060	0.097	0.014	0.182
B cations	1.000	1.000	1.000	1.000	1.000	1.000	1.000	1.000	1.000	1.000	1.000	1.000	1.000	1.000	1.000	1.000
Σ cations	1.985	1.972	1.995	1.716	1.906	1.880	2.026	2.031	1.982	1.895	1.860	1.949	2.260	2.305	2.052	2.029

Note. alt – altered part, bd – below detection limit, na – not analyzed.

balance, showed the proportions of O and OH in the anion site for EM fergusonite-(Y) in the range $O_{3.15}OH_{0.85}$ to $O_{2.34}OH_{1.66}$. On the classification diagram of Ercit (2005) altered fergusonites clearly show an upper-left shift from their unaltered hosts (Fig. 4b), suggesting a combination of such processes as hydration, *A*-cation loss and the addition of Si, Fe, Al, and to some extent Ca. All these alteration trends are

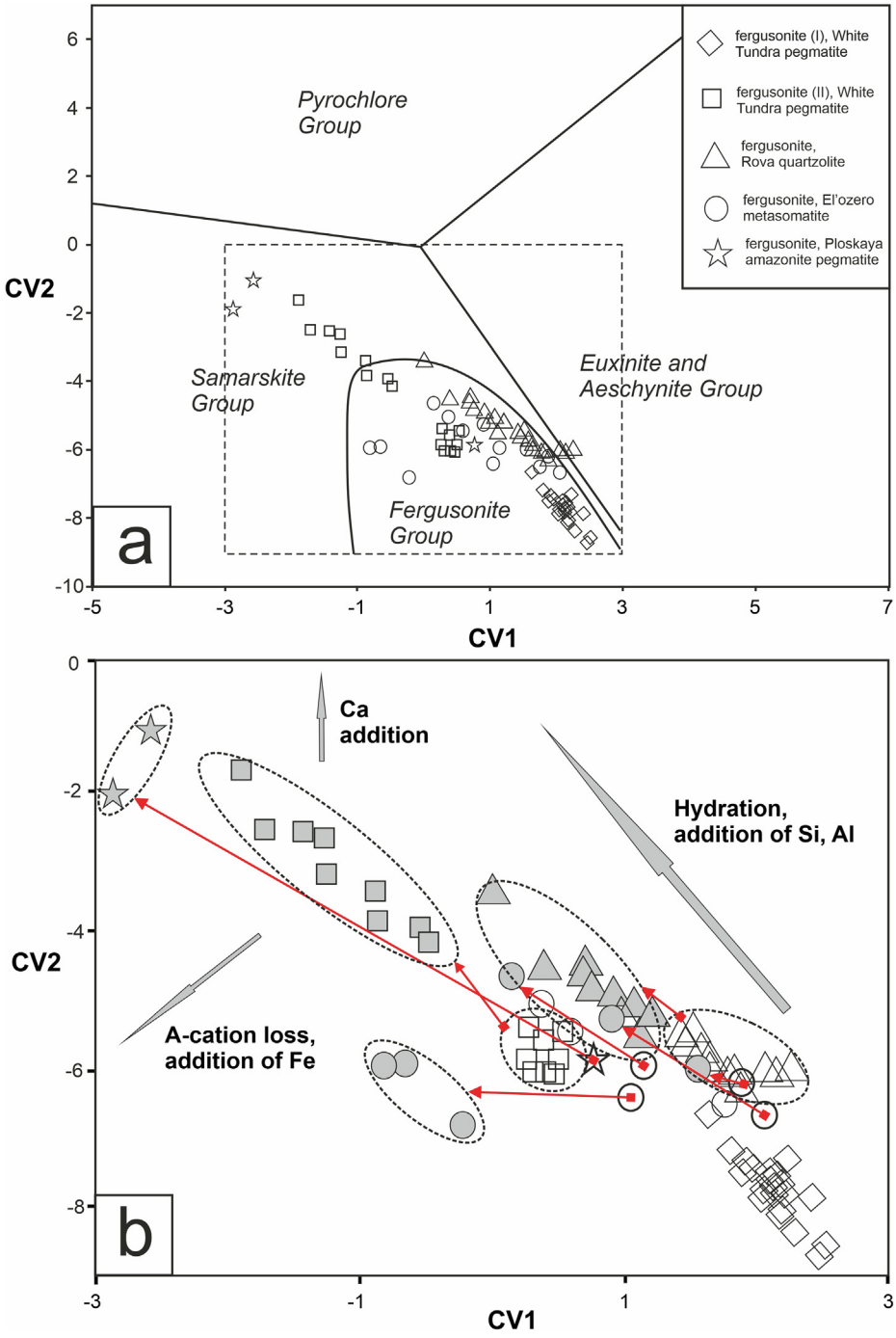

Fig. 4. (a) Fergusonite-(Y) from Keivy rare-metal rich lithologies plotted as canonical variables CV1 and CV2 of the three-group model of Ercit (2005). CV1 = 0.245Na + 0.106 Ca – 0.077 Fe* + 80.425 Pb + 0.220 Y + 0.280 LREE + 0.137 HREE + 0.100 U* + 0.304 Ti + 0.097 Nb + 0.109 Ta* −12.81 (oxide wt.%). CV2 = 0.102Na – 0.113 Ca – 0.371 Fe* − 0.167 Pb – 0.395 Y – 0.280 LREE – 0.265 HREE – 0.182 U* − 0.085 Ti – 0.166 Nb – 0.146 Ta* + 17.29 (oxide wt.%). Fe* = Fe + Mn; U* = U + Th; Ta* = Ta + W. (b) Enlarged box from Fig. 4a showing the difference between unaltered (empty symbols) and altered (filled symbols) fergusonites; red arrows connect altered fergusonites-(Y) and their unaltered hosts; the overall geochemical trends of alteration are shown (grey arrows). (For interpretation of the references to colour in this figure legend, the reader is referred to the web version of this article.)

directed towards the samarskite field, a few analyses falling into the field. Grigoriev and Sergeeva (1993) described late samarskite replacing fergusonite-(Y) from the Aryskan deposit in the Sayany Mts. The theoretical simplified formula of samarskite-(Y), $YFe^{3+}Nb_2O_8$ (Britvin et al., 2019), needs about 0.5 apfu of Fe (according to the formula calculation adopted here) which is much higher than those values in the Keivy minerals. Thus we prefer to use the term altered fergusonite for these analyses.

The alteration trends of Keivy fergusonite are generally in agreement with earlier studies. Ruschel et al. (2010) reported broadly comparable chemical alteration patterns in fergusonite from the Berer region, Madagascar, namely enrichment in SiO_2 (even higher values up to 9.38 wt%) and CaO (up to 7.72 wt%) and depletion in Y_2O_3 (to 6.39 wt %), and also related the changes to interaction with fluids. Tomašić et al. (2006) reported, in a mineral from Ytterby, Sweden, a water content of 8.12 wt% and considerable variation in the *A*-site cations, especially Ca, Fe and Y.

A chondrite-normalised plot (Fig. 5) shows that the fergusonite-(Y) in all occurrences is LREE-depleted and HREE + Y-enriched, with a strongly unfractionated pattern for the LREE ($[La/Gd]_n$ = 0.01–0.07) and a mostly flat pattern for HREE ($[Gd/Lu]_n$ = 0.1–1.2). Significant positive Eu anomalies (Eu/Eu* 1.6–2.4) are observed for the mineral from RQ, EM and PAP, while the WTP fergusonite-(Y) I has Eu below detection limit. The persistent negative anomaly at Yb has not, so far as we know, been previously recorded in fergusonite (e.g. Gieré et al. (2009), Uher et al. (2009), Ruschel et al. (2010), Prol-Ledesma et al., 2012).

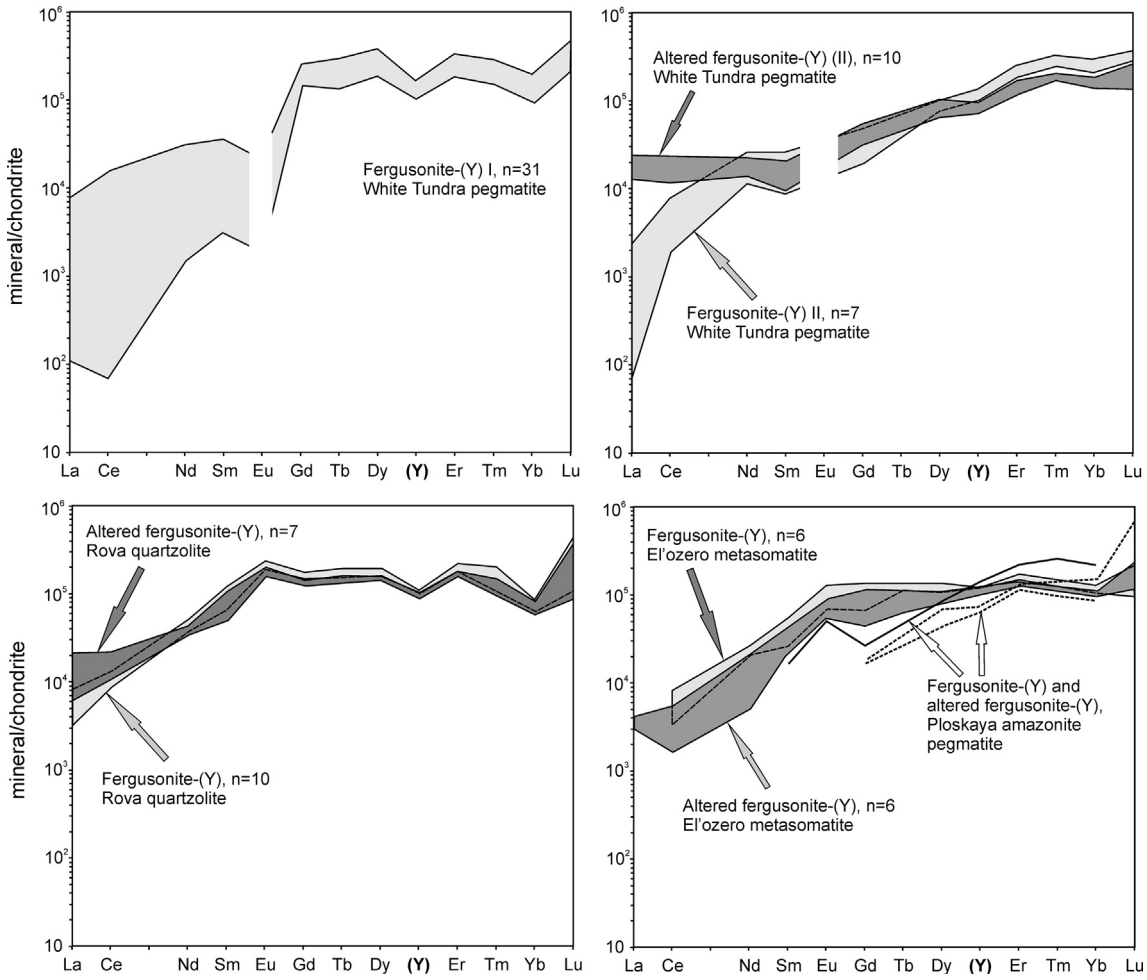

Fig. 5. Chondrite-normalized REE patterns for fergusonite-(Y) from rare-metal rich lithologies related to the Keivy alkali granite complex. Normalizing factors from Sun and McDonough (1989).

5. Discussion

5.1. REE and Nb enrichment processes in the Keivy alkali granite complex

REE and Nb are considered to be incompatible elements, with Nb being more incompatible than REE, especially the HREE and Y. Another geochemical difference between REE and Nb is that REE act as cations, whereas Nb form the nuclei of complex anions (Möller, 1989). That is why the largest Nb deposits tend to be formed by magmatic processes (e.g. in carbonatite complexes), whereas hydrothermal and metasomatising fluids play a significant role in the formation of world-class REE deposits.

The strong enrichment in REE and HFSE characteristic of alkali granite – syenite complexes and their products can be related to two processes: enrichment through extended fractional crystallization of alkaline magmas and enrichment *via* late- and post-magmatic processes with the involvement of pegmatitic and hydrothermal fluids (Boily and Williams-Jones, 1994; Schmitt et al., 2002; Salvi and Williams-Jones, 2005, 2006; Sheard et al., 2012; Dostal et al., 2014; Linnen et al., 2014).

High $[La/Yb]_n$ ratios, deep negative Eu anomalies, extremely high values of the Fe-index (90–100%), and low Ca contents are characteristic of the Keivy alkali granite and imply that the rocks were formed by protracted fractional crystallization (Zozulya et al., 2012, 2005). One possible fractionated phase is Ca-rich plagioclase. Its removal increased alkalinity and lowered Al in residual melts, and might be the reason for the formation of the associated coeval gabbro-anorthosite bodies. This process was mainly responsible for the enrichment of the Keivy granite and its late-magmatic products in Nb (Table 3); the granite and mineralized granite have 2 and 4 times OIB (Sun and McDonough, 1989), respectively.

Undoubtedly, the dominant processes in the enrichment of the REE (especially HREE) and Y in the late- and post-magmatic products of the Keivy complex was hydrothermal activity. It has been established by numerous theoretical studies (Wood, 1990, 2005; Hass et al., 1995; etc.) that the REE form the most stable complexes with F and moderately strong and/or weaker complexes with CO_3^{2-}, SO_4^{2-} and Cl^- (Samson and Wood, 2005). Thus, REE fluoride complexes are the main agents for transporting and precipitation of REE by fluids derived from alkaline magmas, initially enriched in F and REE.

Keivy mineralized granites, quartzolites and metasomatic rocks show unfractionated chondrite-normalized HREE patterns, sometimes with U-type shapes (Table 3; Fig. 6). Empirical and experimental data (Kosterin, 1959; Mineev, 1963; Mineev, 1968; Taylor et al., 1981; Charoy and Raimbault, 1994) have shown that a selective accumulation of HREE in late- and post-magmatic rocks is promoted by high contents of alkalis (mainly sodium), fluorine, and CO_2 in metasomatizing or hydrothermal fluid/solutions. This agrees with the inferred scheme of evolution of the Keivy rocks: silicification (granite-related process), albitization (syenite-related process) and crystallization of hydrothermal minerals (fluorite, carbonates, zeolite group minerals) at the late- and post-magmatic (including pegmatitic) stages of massif formation have been established by petrographic studies and zircon mineralogy (Batijeva, 1976; Batieva and Bel'kov, 1984; Lyalina et al.,

Table 3
Bulk chemistry in selected whole-rock samples of the Keivy alkali granite complex and related rare-metal rich lithologies.

Sample	1	2	3	4	5	6
Rock	aegirine-arfedsonite granite	aegirine-arfvedsonite granite	mineralised granite	quartzolite	quartzolite	apobasic metasomatite
Massif	W.Keivy	White Tundra	W.Keivy	W.Keivy	W.Keivy	El'ozero
wt.%						
SiO_2	73.9	72.2	75.5	61.0	67.3	25.9
TiO_2	0.15	0.37	0.31	1.77	2.35	5.48
Al_2O_3	10.25	11.60	7.91	5.53	1.74	6.43
FeO_t	5.60	5.30	7.93	14.25	10.29	7.46
MnO	0.087	0.077	0.085	0.360	0.130	0.33
MgO	0.036	0.070	0.040	0.240	0.070	0.38
CaO	0.10	0.37	0.19	2.55	1.17	6.72
Na_2O	4.89	4.02	2.46	4.01	2.90	0.14
K_2O	4.16	5.07	4.10	0.88	0.56	0.32
H_2O^-	0.04	0.20	0.08	0.10	0.17	1.17
LOI	0.70	0.43	0.49	0.64	0.85	5.3
P_2O_5	0.03	n.a.	0.01	0.46	0.11	0.05
F	0.063	0.039	0.067	0.370	0.033	0.32
Cl	na	0.004	na	na	0.010	0.032
CO_2	na	0.040	0.040	0.140	0.040	0.1
ppm						
Nb	45	63	97	14.300	240	61.830
Zr	977	1340	5200	48.000	2570	66.700
Y	36	91	106	4570	19.600	42.130
La	51	112	330	786	2840	14.920
Ce	98	257	530	2000	7240	30.450
Pr	na	na	60	270	1085	3250
Nd	46	105	218	1190	4180	9690
Sm	9.09	21.56	46	590	1360	2670
Eu	0.60	1.43	1	41	157	155
Gd	9.3	17.9	30	920	1960	3560
Tb	1.51	2.91	9	190	480	870
Dy	na	na	66	1430	3440	6710
Ho	na	na	49	380	790	1570
Er	na	na	59	800	2430	5420
Tm	1.14	1.55	25	123	480	760
Yb	8.30	11.10	100	878	4120	4220
Lu	1.25	1.53	na	27	107	430

Note. Analyzed by wet chemistry methods (oxides, F, Cl) and XRF (elements) in GI KSC RAS. Apatity. REE for samples 1 and 2 analyzed by INAA in University of Lowell, Lowell, Massachusetts. na = not analyzed.

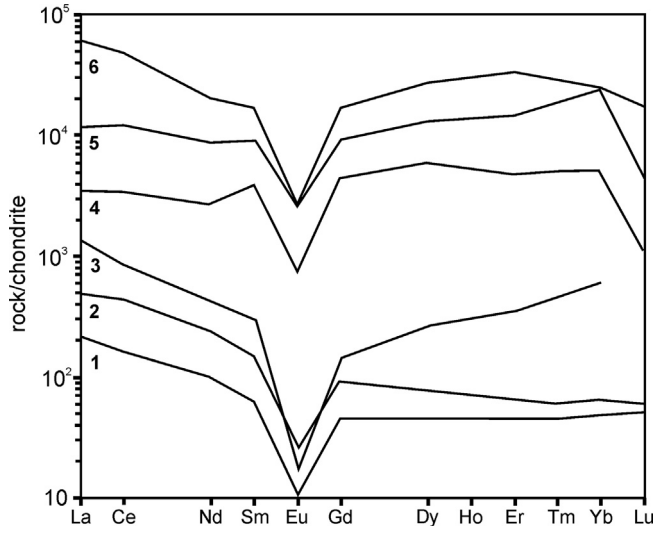

Fig. 6. Chondrite-normalized REE patterns for alkali granites and related REE-rich lithologies of the Keivy complex:1 – West Keivy alkali granite; 2 – White Tundra alkali granite; 3 – West Keivy mineralized granite; 4 – fergusonite-zircon quartzolite; 5 – britholite-zircon quartzolite; 6 – quartz-epidote (apobasic) metasomatite. Normalizing factors from Sun and McDonough (1989).

2010; Zozulya et al., 2012). The different degrees of autometasomatic and fluid reworking of the rocks and their significant role in the ore varieties is emphasized by their higher F contents and positive correlation between Na_2O and HREE (Zozulya et al., 2012, 2015, 2019). In addition, the mineralized granite and nepheline syenite have much higher U and Th contents and Th/U ratios (Zozulya et al., 2012), which are also related to late fluid reworking. The predominant accumulation of Th in the ores indicates a high alkali content and a significant prevalence of F over CO_2 in the ore-forming fluid (Keppler and Wyllie, 1990). Similar Th behavior with respect to U has been noted for many magmatogenic REE deposits that were subjected to intense reworking by hydrothermal alkaline-fluorine fluids (Trueman et al., 1988; Charoy and Raimbault, 1994). It is suggested that partitioning of F into fluid is also promoted by a low Ca content in the melt.

There is a little information on the solubility of Nb in late-magmatic and hydrothermal fluids. Nevertheless it has been predicted that Nb may form complexes with fluoride and may be soluble at high pH with the formation of hydrolyzed anionic species (Wood, 2005). Indeed, a number of geological observations and geochemical studies provide good evidence for Nb enrichment in hydrothermal environments, along with Zr and REE, and in alkali granite-syenite related deposits (e.g. Thor Lake; Trueman et al., 1988; Strange Lake; Salvi and Williams-Jones, 1996; Haldzan Buregtey; Kempe et al., 1999).

Compositional studies of britholite-group minerals from the rare-metal rich products of the Keivy alkali granite (mineralized granite, pegmatite, quartzolite, metasomatite) point to similar fluid

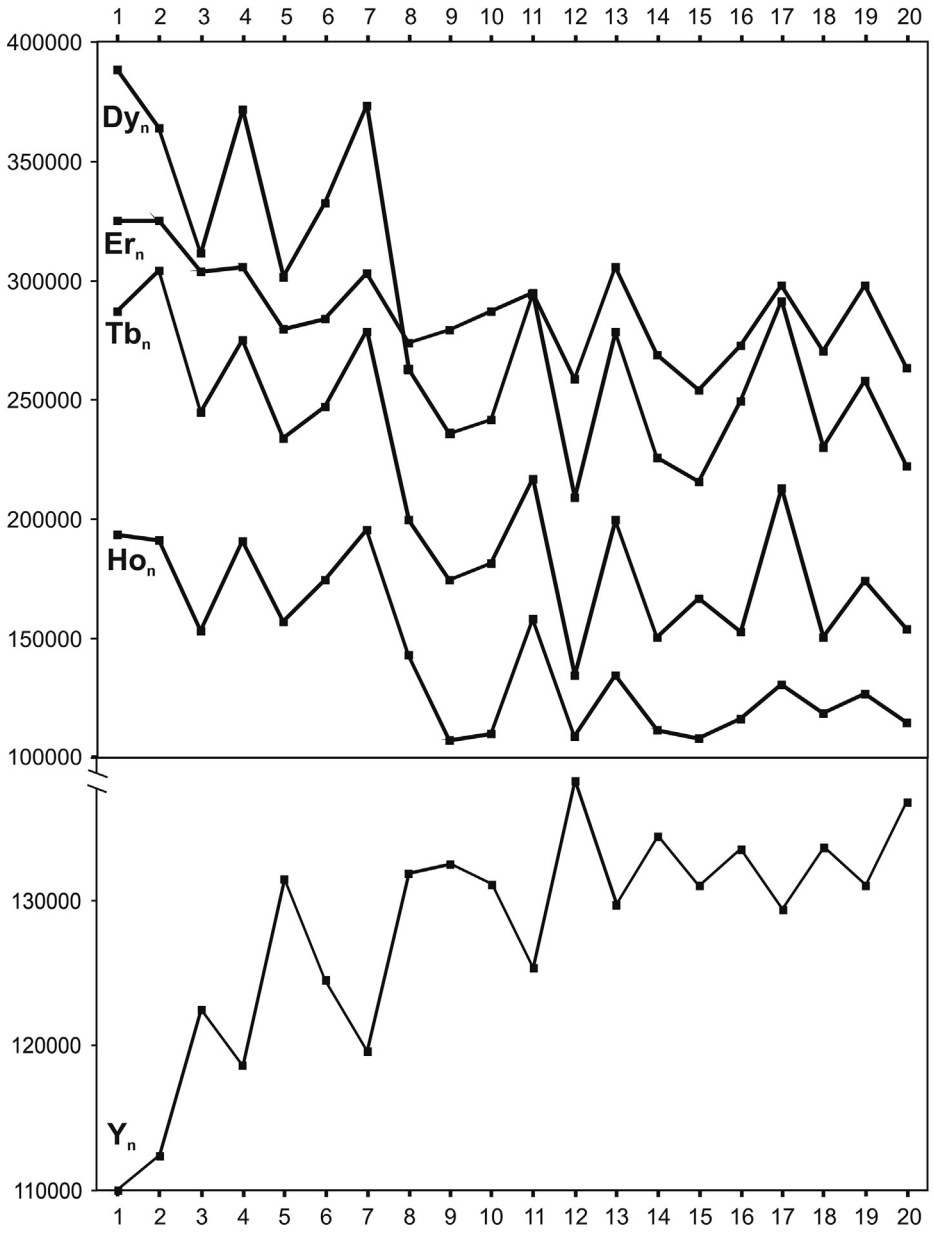

Fig. 7. Chondrite-normalized contents of Y and selected REE with nearly identical ionic radii (Tb, Dy, Ho, Er) along the profile 1–20 in fergusonite-(Y) I from the White Tundra pegmatite (Fig. 3a). Normalizing factors from Sun and McDonough (1989).

characteristics (Zozulya et al., 2019). Fluorbritholite-(Y) and britholite-(Y) from the White Tundra pegmatite and the Rova quartzolite formed under relatively high F activity in fluids with low CO_2/H_2O ratios. The highly variable F content (from highest to lowest after precipitation of abundant fluorite) and comparatively elevated CO_2/H_2O ratios are inferred for metasomatizing fluids emanating from alkali granitic magma, which affected the basic country rocks in the El'ozero occurrence, with crystallization of fluorbritholite-(Ce).

Whole-rock geochemical and mineralogical data indicate that the hydrothermal fluids emanating from the Keivy alkaline magmas were mainly alkaline and F-rich, with changing proportions of H_2O and CO_2. The role of other possible ligands (Cl, S) in the mobilization of the REE was unimportant due to their negligible concentrations in the parental alkali granite (Cl $\leq$ 0.01 wt%, S $\leq$ 0.1 wt%) and the absence of evidence that they were introduced during post-magmatic processes.

5.2. REE fractionation during crystallization of fergusonite-(Y): the role of changing fluid composition

The usual interpretation of the geochemical properties of REE (with the exceptions of Eu and Ce due to their possibly heterovalent state) is mainly based on the size of the ionic radii. The radii increase from Y^{3+} to La^{3+}, and decrease from Y^{3+} to Lu^{3+}, due to the lanthanide contraction. As a consequence, the ionic radii of the HREE are similar to that of Y, and the closest crystal-chemical similarity and geochemical behavior should be shown by Tb, Dy, Ho and Er, whose radii are nearly identical to that of Y. Nevertheless, Tb, Dy, Ho, Er, and to a lesser extent Gd, show reciprocal (oscillatory) distributions with Y in fergusonite-(Y) I from the White Tundra pegmatite along profile 1–20 (Fig. 7). Coupled with the fact that the abundances of all these elements decrease with increasing Y, a strong substitution relationship between Y and Tb, Dy, Ho, Er, Gd could be suggested. To our knowledge, such a reciprocal distribution is one of the best parameters found before in REE minerals and depends of the specific conditions of pegmatite formation. The REE

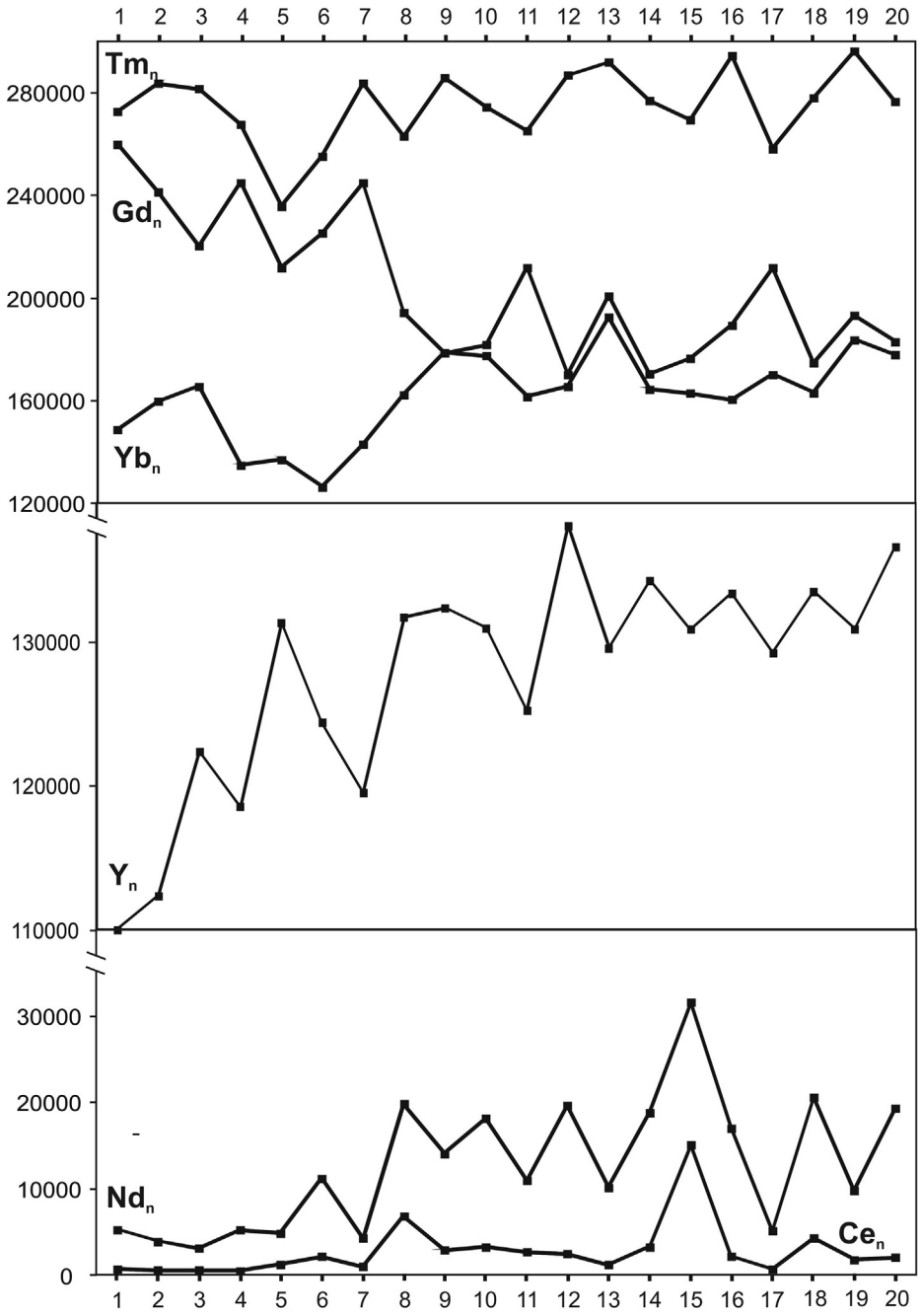

Fig. 8. Chondrite-normalized contents of Y and selected REE with very different ionic radii (Ce, Nd, Gd, Tm, Yb) along profile 1–20 in fergusonite-(Y) I from the White Tundra pegmatite (Fig. 3a). Normalizing factors from Sun and McDonough (1989).

with very different ionic radii, such as Ce, Nd, Tm, Yb, show no reciprocal distribution with Y along profile 1–20 (Fig. 8), showing no tendency to substitute for Y. A possible explanation of the negative correlation between Y and Tb, Dy, Ho, Er is a change in crystallization conditions during the formation of the fergusonite-(Y) I. It is known from a number of experimental and theoretical studies that all the REE form complexes with F but with different solubilities (London et al., 1988; Keppler, 1993; Migdisov et al., 2009). The important role of REE-F complexes in the formation of REE-F-rich granite-related deposits has been extensively studied by a number of authors (Bilal and Becker, 1979; Bilal et al., 1979; McLennan and Taylor, 1979; Bilal and Kob, 1980; Salvi and Williams-Jones, 1996; Williams-Jones et al., 2000; Agangi et al., 2010).

For example, Y fluoride complexes are more stable than Dy fluoride complexes; the stability constant for YF^{2+} ($\log_{10}$ K = 4.80) is nearly three times as high as the corresponding complex of Dy ($\log_{10}$ K = 4.36) (Brookins, 1989; Gramaccioli et al., 1999). Fluorine enrichment during crystallization will result in successive increases of the Y/Dy ratio in the fluid until crystallization of F-rich minerals (normally fluorite, in some cases fluorapatite) occurs. The consumption of F destabilizes the Y-F complexes, resulting in the local crystallization of REE minerals with higher Y/Dy ratios. At that stage, Dy will tend to enter any REE minerals formed more efficiently than Y. Applied to fergusonite-(Y) I from the White Tundra pegmatite, the Y/Dy ratio shows an overall tendency to rise from point 1 (Y/Dy = 1.8) to point 20 (Y/Dy = 3.9) along the profile (Fig. 9). This points to the lowering of the F concentration in the fluid during crystallization. Of interest is the same distribution of Y/Er ratio, with a rise from 3.5 to 5.1, which indicates a

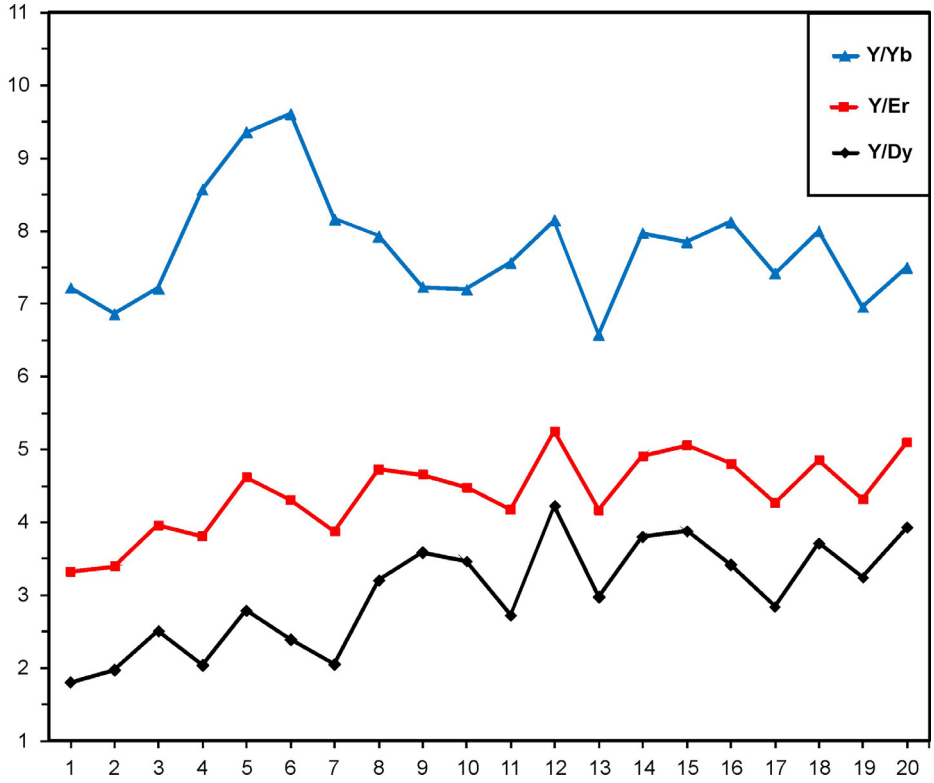

Fig. 9. Y/Dy, Y/Er and Y/Yb distributions along profile 1–20 in fergusonite-(Y) I from the White Tundra pegmatite.

similar behavior of the Y-Er pair with a changing F content. In contrast, the distribution of the Y/Yb ratio is different from that of Y/Dy (Fig. 9), as Y and Yb have very different ionic radii. Apparently, the pegmatitic crystallization environment favored the prolonged crystallization of coarse grains of fergusonite-(Y) I. Unfortunately, it is difficult to be specific about the temporal evolution of F activity during crystallization, as the zoning with the Y/Dy change is asymmetrical. Nevertheless, a similar zoning pattern in two neighboring crystals (Fig. 3a) points to a gradient of F concentration in this part of the pegmatite that was recorded in the composition of the fergusonite-(Y).

A weak negative correlation between Y and Dy and an insignificant change in Y/Dy (from 3.53 to 3.97) are found in rare discrete grains of unaltered fergusonite-(Y) from the quartzolite (i.e. analysis points 1, 2, 3, 4, 5, sample 1–93, Table 1, Supplementary Table 2S). The zoning is irregular and patchy, pointing rather to a substitution mechanism than to a change of fluid composition.

5.3. Behavior of REE during alteration of fergusonite-(Y): the role of changing fluid composition

As a loss of *A*-site cations is one of the alteration trends in Keivy fergusonite-(Y) (Section 4.2), it is important to investigate the relative behavior of Y and the REE during this loss. Altered fergusonite-(Y) from all occurrences shows significant loss of Y (from ≈10% for minerals from the Rova quartzolite and El'ozero metasomatite to ≈30–50% for minerals from the White Tundra pegmatite and Ploskaya amazonite pegmatite (Fig. 10). The individual REE behave differently. Heavy REE show almost the same behavior as Y. There are decreases of Dy and Ho in the altered phases but of lesser magnitude than Y, about 5–10% for RQ, EM and PAP, and no decreases in WTP. Losses of Er and Yb are of the same magnitude as for Y in WTP, PAP and EM, with no loss of Yb in RQ. As a whole, with rare exceptions (possibly due to analytical errors), the HREE decrease during alteration, which can be simply explained by their similar properties to Y.

The LREE also show differences. Neodymium decreases slightly in RQ and EM, with no or slight increases in WTP. Cerium increases in the altered products of RQ and WTP fergusonite-(Y) (up to ≈50% in WTP). However, it is lower in EM and no Ce is detected in PAP. There are two possible explanations for the Ce increase. Cerium is extremely incompatible and tends to accumulate in late derivatives; thus the alteration fluids should be more enriched in Ce. The other explanation is that the F enrichment in the fluid/solution affected the fergusonite-(Y). YF^{2+} complexes are more stable in hydrothermal fluids than CeF^{2+}, the YF^{2+} stability constant being nearly five times higher than the corresponding Ce complex (Brookins, 1989; Gramaccioli et al., 1999)). That is why a high F content in the fluids favors the inferred precipitation of relatively Ce-rich altered fergusonite. On the other hand, this explanation agrees with Ce lowering in fergusonite-(Y) from EM and PAP, for which a low F content in the fluids has been inferred (Section 5.5).

As Y, REE and Nb in fergusonite-(Y) can be mobilized during alteration, their relative mobilities are important controls of their redistribution patterns. Evidence has been found in expansion cracks around fergusonite-(Y) from RQ described by Macdonald et al. (2017). The cracks are 10–15 μm wide and a few mm long (Fig. 2a), starting on the boundary of fergusonite-(Y) grains and terminating in quartz. The cracks are dominated by Nb, U, Pb and REE, with lesser amounts of Th, Si and Fe, and have low analytical totals (75–93 wt%) (Supplementary Table S3). The proportions of the main components are variable. Some cracks are rich in U (27–35 wt% UO_2) and low in REE + Y (3.6–5.3 wt % oxides); others are rich in REE + Y (12–25 wt% oxides) and low in U (1.4–2.4 wt% UO_2). PbO ranges from 13 to 27 wt%. However, the persistent enrichment in Nb (20–34 wt% Nb_2O_5) and spatial proximity to fergusonite-(Y) suggest that the main component filling the cracks is from the fergusonite-(Y). Chondrite-normalized REE patterns are rather flat (Fig. 11), with $[La/Yb]_n$ varying from 1.5 to 4.3, and with strong Ce enrichment relative to the other LREE (Ce/Ce* 1.0–5.6). The textural relationships between the cracks and fergusonite-(Y) do not permit recognition of the temporal sequence between crack formation and the alteration of fergusonite-(Y), i.e. whether the cracks are products of metamictization or alteration or both. The hydrous nature of the cracks,

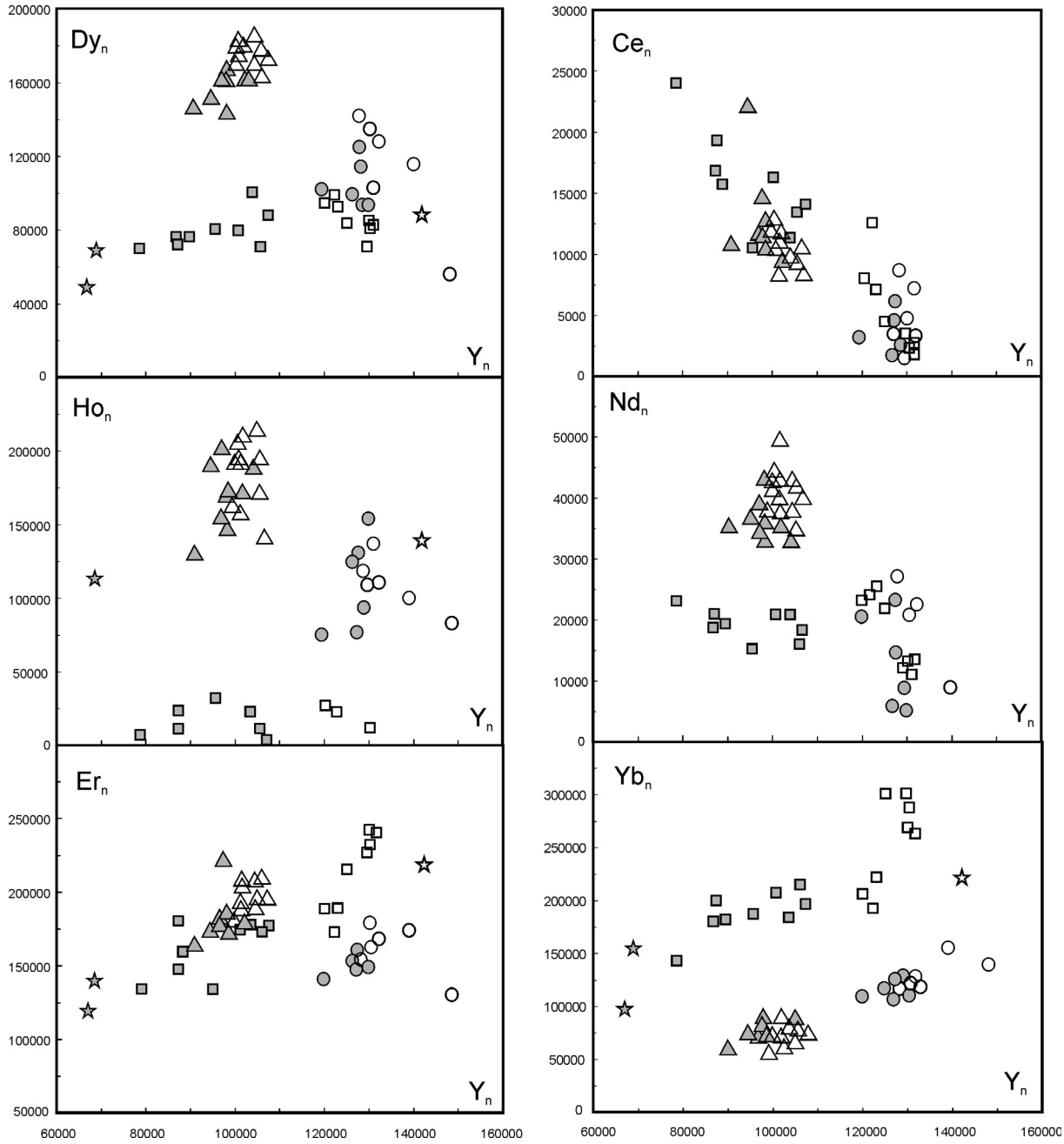

Fig. 10. Y *vs* selected REE plot for fergusonite-(Y) from various rare-metal rich lithologies of the Keivy alkali granite complex, showing the distributions of unaltered and altered species. Same symbols as in Fig. 4.

the Ce enrichment coupled with lower HREE, and the high and similar U contents in the altered and unaltered RQ fergusonite-(Y) point to a governing role of fergusonite alteration in the formation of the cracks.

Actinide concentrations in fergusonite-(Y) from all groups may provide interesting information about alteration controls. Uranium and Th concentrations are lowest in fergusonite-(Y) I from WTP (0.001–0.008 apfu and 0.005–0.02 apfu, respectively). High U and Th contents are observed in unaltered and altered fergusonite-(Y) II from WTP, RQ, EM and PAP (0.012–0.039 apfu and 0.005–0.038, respectively). We suggest that the higher actinide contents in fergusonite-(Y) II from WTP, RQ, EM and PAP compared to fergusonite-(Y) I from WTP made them more prone to alteration due to radiation damage.

5.4. Nature of the positive Eu/Eu* anomaly in fergusonite

As the Keivy alkali granite is a product of protracted fractional crystallization, it has a prominent negative Eu/Eu* anomaly (Fig. 6, Section 5.1) due to the removal of calcic plagioclase. The same anomaly is observed in late- and post-magmatic bodies related to the granite (e.g. quartzolite, metasomatite). It might, therefore, be expected that the REE-minerals from mineralized lithologies would also show negative Eu/Eu* anomalies. However, the fergusonite-(Y) from the Rova quartzolite, the El'ozero metasomatite and the Ploskaya amazonite pegmatite (with the exception of the White Tundra pegmatite) has positive Eu/Eu* anomalies. The same pattern is present in altered fergusonite-(Y) from the Rova and El'ozero occurrences. Increasing oxidation and a change of Eu^{2+} to Eu^{3+} seem unlikely, as Eu^{3+} has an ionic radius (1.2 Å) sufficiently larger than Y (0.9 Å) to preclude

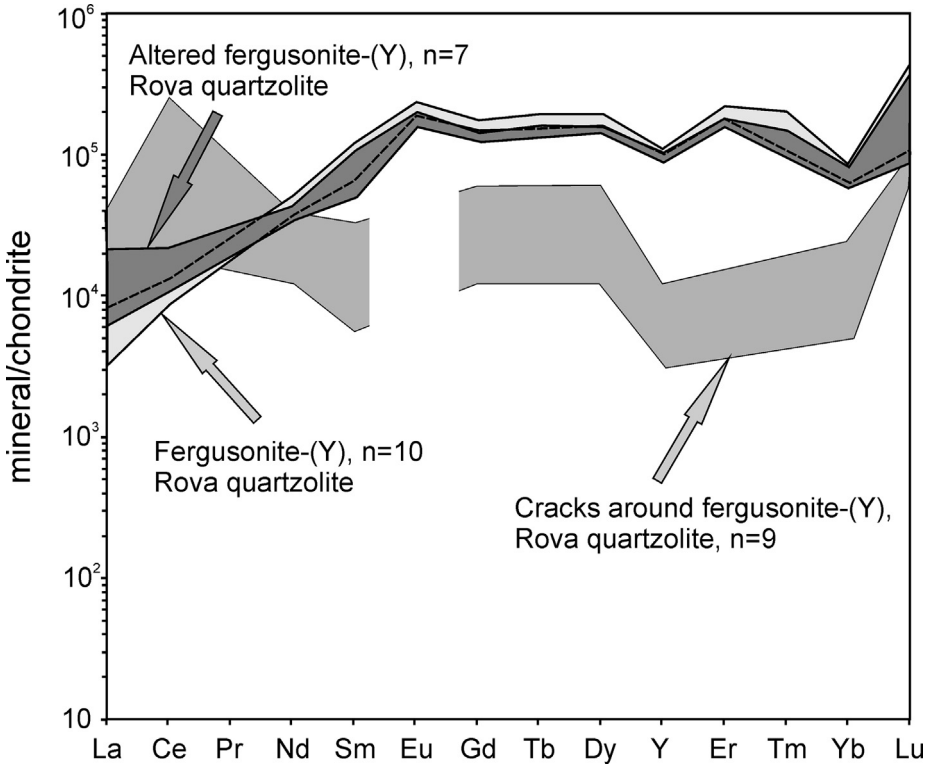

Fig. 11. Chondrite-normalized REE patterns for fergusonite-(Y) and expansion cracks around fergusonite-(Y) from the Rova quartzolite. Normalizing factors from Sun and McDonough (1989).

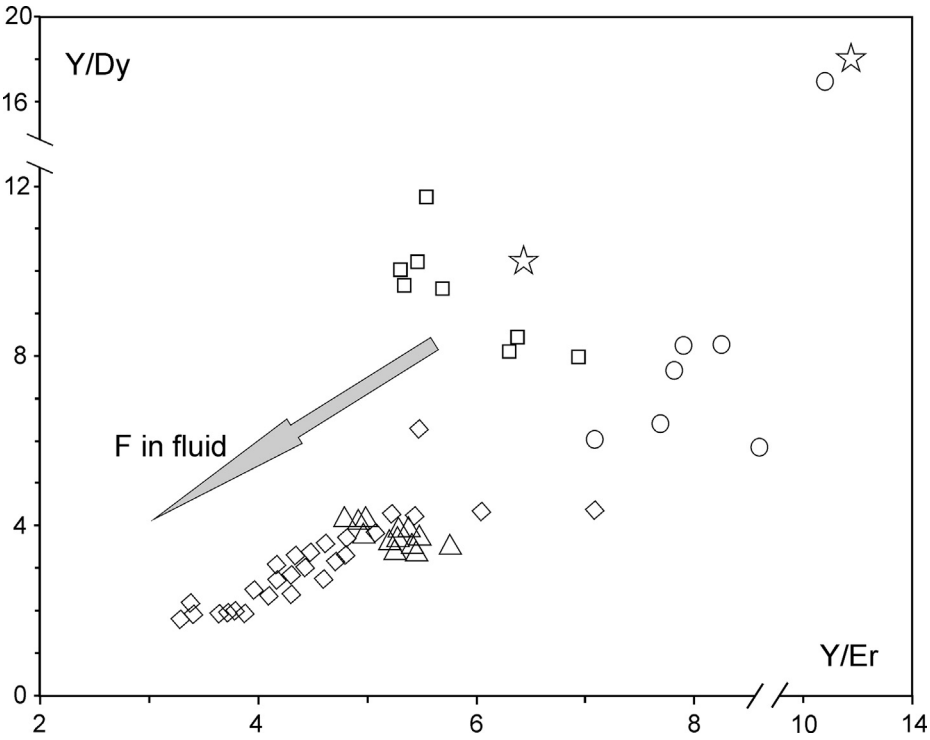

Fig. 12. Y/Er *vs* Y/Dy plot for unaltered fergusonite-(Y), illustrating the relative F activity in fluids of various rare-metal rich lithologies of the Keivy alkali granite complex. Same symbols as in Fig. 4.

substituting for it significantly. Moreover, the overall Eu concentrations in quartzolite, metasomatite and amazonite pegmatite systems, if they are closed, must remain negligible. In the cases discussed here, an external source of the Eu appears to be necessary. All the above mentioned occurrences are emplaced into (metasomatite, amazonite pegmatite), or located in close vicinity to (quartzolite), country rocks (metavolcanic and intrusive intermediate-basic rocks). Fluids emanating from the granite interacted with them, resulting in the breakdown of Ca-plagioclase, mainly by sericitisation and albitization, with the liberation of Eu which entered the fluid. A similar process was

suggested to explain the formation of late REE-bearing epidote extremely enriched in Eu from the Tatyana pegmatite, Haldzan Buragtag massif, Mongolian Altai (Kartashov et al., 1993). The selective extraction into solution of Eu relative to neighboring REE during low-temperature basalt-water interaction has been confirmed by experimental studies (Nakada et al., 2017). The twofold to tenfold enrichment of fergusonite-(Y) in the middle and heavy REE relative to other REE-bearing minerals from the study occurrences explains the presence of positive Eu/Eu* anomalies in fergusonite and the concurrent lack of the same anomaly in britholite, chevkinite, monazite, allanite (Bagiński et al., 2016; Macdonald et al., 2017; Zozulya et al., 2019). The suggested mechanism of Eu enrichment in fergusonite from Rova, El'ozero and Ploskaya is indirectly confirmed by the presence of a profound negative Eu/Eu* anomaly in fergusonite-(Y) from the White Tundra pegmatite which occurs in a granite mass far from the country rocks.

5.5. REE variations in fergusonite as indicators of fluid composition in Keivy rare-metal occurrences

An analysis of REE variations in fergusonite can be regarded as a useful tool in the estimation of the proportions of the main ligands in the fluids, i.e. F, CO_2, H_2O. In addition to the Y/Dy ratio, mentioned above, the $[La/Nd]_n$ and Y/Er ratios provide relevant information.

Smith et al. (2000) showed that the fractionation of La from Nd depends on the CO_2 content in the mineral-forming solutions which affects the $[La/Nd]_n$ ratio in REE minerals (> 4 for CO_2-rich solution, < 4 for H_2O-rich solution). Since the paragenetic environment studied in Smith et al. (2000) differs from those of the Keivy occurrences, the conclusions given below are indirect. The $[La/Nd]_n$ ranges from 0.03 to 1.2 in fergusonites from all the occurrences, pointing to a relatively high H_2O/CO_2 ratio in their fluids during the crystallization of fergusonite. One possible reason is the consumption of CO_2 during the earlier crystallization of carbonates. The White Tundra pegmatite provides good evidence of this process, where the mass crystallization of kainosite-(Y) predated the formation of fergusonite-(Y).

The use of the Y/Dy ratio coupled with Y/Er provides information on the duration of formation of a given REE mineral, the change of F composition in the fluid phase during crystallization, and the difference in F activity in fluids in lithologies formed by various genetic processes. Erbium has a similar ionic radius and ErF^{2+} stability constant to Y (Gramaccioli et al., 1999). There are decreases in the Y/Er ratio with increases of F in the crystallization environment. Fergusonites from the Keivy occurrences studied here have different ranges of Y/Dy and Y/Er ratios. Y/Dy varies from 2 to 4 in fergusonite-(Y) I from WTP, from 7 to 12 in fergusonite-(Y) II from WTP, from 3 to 4 in RQ, and from 5 to 8 in EM. The highest Y/Dy is observed in fergusonite-(Y) from PAP (10 and 17). The ranges of Y/Er are 3–6 in fergusonite-(Y) I from WTP, from 5 to 7 in fergusonite-(Y) II from WTP, 5–6 in RQ, 7–9 in EM. Again the highest Y/Er ratios are in PAP (6 and 13). On a Y/Er *vs* Y/Dy plot (Fig. 12) the different groups of Keivy fergusonite-(Y) have discrete populations. Fergusonite-(Y) I from WTP formed at the highest F activity, while fergusonite-(Y) II from the same occurrence formed at moderate F activity. Thus these groups record different stages of WTP evolution. Moreover, fergusonite-(Y) I crystallized with a gradual change of F content in the fluid, assuming a relatively prolonged period of growth. A change of fluid composition and a multistage evolution are common features of pegmatite formation (London, 1987, 2008; Simmons and Webber, 2008; Linnen et al., 2012; etc.). Fergusonite-(Y) from RQ formed at relatively high to moderate F activity. A low activity of F in the fluid is characteristic of the crystallization of fergusonite-(Y) in EM and PAP. Apparently, their high Ca content favored extensive precipitation of fluorite and bonding of F.

6. Conclusions

(1) Five groups of fergusonite are distinguished on the basis of internal textures and lithology: fergusonite-(Y) I and fergusonite-(Y) II from the White Tundra pegmatite; fergusonite-(Y) from the Rova quartzolite; fergusonite-(Y) from the El'ozero metasomatite; fergusonite-(Y) from the Ploskaya amazonite pegmatite. Fergusonite-(Y) I from the White Tundra pegmatite is unaltered, while those in other groups were prone to alteration.
(2) Fergusonite-(Y) I from the White Tundra pegmatite has a negative correlation of Y with Tb, Dy, Ho, Er along a profile through the grain. This REE fractionation during crystal growth is explained by changes of the F content in the fluid.
(3) The main alteration trends of Keivy fergusonite-(Y) were hydration, addition of Si, Al and Fe, and *A*-cation loss. The loss of Y and HREE and addition of Ce during alteration of fergusonite-(Y) from the White Tundra pegmatite and the Rova quartzolite were governed by two major processes: Ce accumulation in late derivatives and the high F content in the crystallization environment. The lower abundances of Ce in altered fergusonite-(Y) from the El'ozero metasomatite resulted from a low F content in the crystallization environment. The extent of alteration possibly depended on the actinide concentration in the fergusonite-(Y). Crystals with high U (> 0.01 apfu) and Th (> 0.02 apfu) were more prone to alteration through radiation damage.
(4) Positive Eu/Eu* anomalies in the fergusonite-(Y) from the Rova quartzolite, El'ozero metasomatite and Ploskaya amazonite pegmatite resulted from external contributions of Eu from the country rocks after the breakdown of plagioclase.
(5) Differences in $[La/Nd]_n$, Y/Dy and Y/Er ratios in fergusonite-(Y) from various rare-metal rich lithologies may reflect their fluid composition. Fergusonite-(Y) formed under low CO_2/H_2O conditions, but changing F activities. A F-rich fluid is inferred for fergusonite-(Y) from the White Tundra pegmatite and the Rova quartzolite, and a low-F fluid is characteristic of minerals from the El'ozero metasomatite and Ploskaya amazonite pegmatite located in country rocks of the granite massifs.

Declaration of Competing Interest

The authors declare that they have no known competing financial interests or personal relationships that could have appeared to influence the work reported in this paper.

Acknowledgments

We are grateful to Beata Marciniak-Maliszewska from the Inter-Institute Analytical Complex at the Institute of Geochemistry, Mineralogy, and Petrology, University of Warsaw, for technical assistance with microprobe analyses. DZ thanks Nelson Eby, University of Lowell, Massachusetts, for help in acquisition of INAA data on granite REE composition. Two anonymous referees are thanked for very helpful journal reviews. This research was funded by Russian Government Grant 0226-2019-0053.

Appendix A. Supplementary data

Supplementary data to this article can be found online at https://doi.org/10.1016/j.oregeorev.2020.103693.

References

Abu Elatta, S.A., 2019. Geology, mineralogy and mineral chemistry of the NYF-type pegmatites at the Gabal El Faliq area, South Eastern Desert, Egypt. J. Earth Syst. Sci. 128, 156. https://doi.org/10.1007/s12040-019-1169-7.
Agangi, A., Kamenetsky, V.S., McPhie, J., 2010. The role of fluorine in the concentration and transport of lithophile trace elements in felsic magmas: insights from the Gawler Range Volcanics, South Australia. Chem. Geol. 273, 314–325. https://doi.org/10.1016/j.chemgeo.2010.03.008.
Bagiński, B., Jokubauskas, P., Domańska-Siuda, J., Kartashov, P., Macdonald, R., 2016a.

Hydrothermal metasomatism of a peralkaline granite pegmatite, Khaldzan Buragtag massif, Mongolian Altai; complex evolution of REE-Nb minerals. Acta Geol. Pol. 66, 473–491. https://doi.org/10.1515/agp-2016-0021.
Bagiński, B., Zozulya, D., Macdonald, R., Kartashov, P.M., Dzierżanowski, P., 2016b. Low-temperature hydrothermal alteration of a rare-metal rich quartz-epidote metasomatite from the El'ozero deposit, Kola Peninsula, Russia. Eur. J. Mineral. 28, 789–810. https://doi.org/10.1127/ejm/2016/0028-2552.
Barth, T., 1927. The structure of risørite. Nor. Geol. Tidsskr. 9, 37–39.
Batijeva, I.D., 1976. Petrology of Peralkaline Granites of Kola Peninsula. Nauka, Leningrad.
Batieva, I.D., Bel'kov, I.V., 1984. Sakharjok Alkaline Massif, Constituent Rocks, and Minerals. Kola Branch USSR Academy of Sciences, Apatity.
Bayanova, T.B., 2004. The Age of Reference Geological Complexes of the Kola Region and Duration of Magmatic Processes. Nauka, St Petersburg.
Bel'kov, I.V., Batieva, I.D., Vinogradova, G.V., Vinogradov A.N., 1988. Mineralization and Fluid Regime of Contact Zones of Alkali Granite Intrusions. Kola Branch USSR Academy of Sciences, Apatity.
Bilal, B.A., Becker, P., 1979. Complex formation of trace elements in geochemical systems – II. Stability of rare earth fluoro complexes in fluorite bearing model systems at various ionic strengths. J. Inorg. Nucl. Chem. 41, 1607–1608.
Bilal, B.A., Hermann, F., Fleischer, W., 1979. Complex formation of trace elements in geochemical systems – I. Potentiometric studies of fluoro complexes of rare earth elements in fluorite bearing model systems. J. Inorg. Nucl. Chem. 41, 347–350.
Bilal, B.A., Kob, V., 1980. Complex formation of trace elements in geochemical systems – 3. Studies on the distribution of fluoro complexes of rare earth elements in fluorite bearing model systems. J. Inorg. Nucl Chem. 42, 629–630.
Boily, M., Williams-Jones, A.E., 1994. The role of magmatic and hydrothermal processes in the chemical evolution of the Strange Lake plutonic complex, Québec-Labrador. Contrib. Mineral. Petrol. 118, 33–47.
Britvin, S.N., Pekov, I.V.,·Krzhizhanovskaya, M.G., Agakhanov, A.A.,·Ternes, B., Schüller, W., Chukanov, N.V., 2019. Redefinition and crystal chemistry of samarskite-(Y), YFe3 + Nb2O8: cation-ordered niobate structurally related to layered double tungstates. Phys. Chem. Miner. 46, 727–741. https://doi.org/10.1007/s00269-019-01034-0.
Brøgger, W.C., 1906. Die Mineralien der Südnorwegischen Granitpegmatitgänge, I. Niobate, tantalate, titanate und titanoniobate. Videnskapsselskapets Skrifter. I. Mat-Naturv. 6, 138–159.
Brookins, D.G., 1989. Aqueous geochemistry of rare earth elements, in: Lipin, B.R., McKay, G.A. (Eds), Geochemistry and Mineralogy of the Rare Earth Elements, Rev. Mineral, vol. 21, pp. 201–225.
Calderwood, M.A., Grguric, B.A., Jacobson, M.I., 2007. Guidebook to the Pegmatites of Western Australia. Hesperian Press, Perth.
Ćerny, P., Ercit, T.S., 2005. The Classification of granitic pegmatites revisited. Can. Mineral. 43, 2005–2026.
Charoy, B., Raimbault, L., 1994. Zr-rich, Th-rich, and REE-rich biotite differentiates in the A-type granite pluton of Suzhou (Eastern China) - the key role of fluorine. J. Petrol. 35, 919–962. https://doi.org/10.1093/petrology/35.4.919.
Dostal, J., Kontak, D.J., Karl, S.M., 2014. The Early Jurassic Bokan Mountain peralkaline granitic complex (southeastern Alaska): geochemistry, petrogenesis and rare-metal mineralization. Lithos. 202–203, 395–412.
Ercit, T.S., 2005. Identification and alteration trends of granitic pegmatite-hosted (Y, REE, U, Th)–(Nb, Ta, Ti) oxide minerals: a statistical approach. Can. Mineral. 43, 1291–1303.
Ervanne, H., 2004. Uranium oxidation states in allanite, fergusonite and monazite of pegmatites from Finland. N. Jb. Mineral. Mh. 7, 289–301.
Estrade, G., Salvi, S., Béziat, D., Rakotovao, S., Rakotondrazafy, R., 2014. REE and HFSE mineralization in peralkaline granites of the Ambohimirahavavy alkaline complex, Ampasindava peninsula, Madagascar. J. Afr. Earth Sci. 94, 141–155.
Gieré, R., Williams, C.T., Wirth, R., Ruschel, K., 2009. Metamict fergusonite-(Y) in a spessartine-bearing granitic pegmatite from Adamello, Italy. Chem. Geol. 261, 333–345.
Gramaccioli, C.M., Diella, V., Demartin, F., 1999. The role of fluoride complexes in REE geochemistry and the importance of 4f electrons: some examples in minerals. Eur. J. Mineral. 11, 983–992.
Grigoriev, A.V., Sergeeva, V.V., 1993. About the replacement of fergusonite with samarskite within albitites of the Aryskan rare-metal deposit. Zapiski VMO 5, 36–39.
Hass, J.R., Shock, E.L., Sassani, D.C., 1995. Rare earth elements in hydrothermal systems: estimates of standard partial molal thermodynamics properties of aqueous complexes of the rare earth elements at high pressures and temperatures. Geochim. Cosmochim. Acta 59, 4329–4350.
Kapustin, Yu.L., 1976. New occurrence of cerium fergusonite in carbonatites. Proc. Mineral. Museum 25, 166–172.
Kartashov, P.M., Voloshin, A.V., Pakhomovsky, Y.A., 1993. On the zonal gadolinite from the alkaline granitic pegmatites of Haldzan-Buragtag (Mongolian Altai). Proc. Russ. Mineral. Soc. 3, 65–79.
Kempe, U., Goetze, J., Dandar, S., Habermann, D., 1999. Magmatic and metasomatic processes during formation of the Nb–Zr–REE deposits Khaldzan Buregte and Tsakhir (Mongolian Altai): Indications from a combined CL-SEM study. Mineral. Mag. 63, 165–177.
Keppler, H., 1993. Influence of fluorine on the enrichment of high-field strength trace-elements in granitic rocks. Contrib. Mineral. Petrol. 114, 479–488. https://doi.org/10.1007/bf00321752.
Keppler, H., Wyllie, P.J., 1990. Role of fluids in transport and fractionation of uranium and thorium in magmatic processes. Nature 348, 531–533. https://doi.org/10.1038/348531a0.
Kobyashev, Yu.S., Nikandrov, S.N., 2007. Minerals of Ural (minerals and species). Kvadrat Press, Ekaterinburg.
Kosterin, A.V., 1959. On possible forms of transfer of rare-earth elements by hydrothermal solutions. Geokhimiya 4, 310–315.
Levin, V.Ya., Ronenson, B.M., Samkov, V.S., Levina, I.A., Sergeev, N.S., Kiselev, A.P., 1997. Alkaline-carbonatitic complexes of Ural. Uralgeolkom, Ekaterinburg.
Linnen, R.L., Samson, I.M., Williams-Jones, A.E., Chakhmouradian, A.R., 2014. Geochemistry of the Rare-Earth Elements, Nb, Ta, Hf, and Zr Deposits, in: Treatise on Geochemistry, 2nd ed., pp. 543–568.
Linnen, R.L., Van Lichtervelde, M., Černý, P., 2012. Granitic pegmatites as sources of strategic metals. Elements 8, 275–280.
London, D., 1987. Internal differentiation of rare-element pegmatites: effects of boron, phosphorus and fluorine. Geochim. Cosmochim. Acta 51, 403–420.
London, D., 2008. Pegmatites. Can. Mineral. Spec. Publ. 10, 1–347.
London, D., Hervig, R.L., Morgan, G.B., 1988. Melt-vapor solubilities and elemental partitioning in peraluminous granite-pegmatite systems - experimental results with Macusani glass at 200 Mpa. Contrib. Mineral. Petrol. 99, 360–373. https://doi.org/10.1007/bf00375368.
Lyalina, L.M., Zozulya, D.R., Bayanova, T.B., Selivanova, E.A., Savchenko, Ye.E., 2012. Genetic peculiarities of zircon from pegmatites of Neoarchean alkali granites of the Kola region. Zapiski RMO 5, 35–51.
Lyalina, L.M., Zozulya, D.R., Savchenko, E.E., 2010. Multiple crystallization of zircon in the Sakharjok rare-earth element–zirconium deposit, Kola Peninsula. Dokl. Earth Sci. 430, 120–124. https://doi.org/10.1134/S1028334X10010265.
Macdonald, R., Bagiński, B., Kartashov, P.M., Zozulya, D., Dzierżanowski, P., 2015. Interaction of rare-metal minerals with hydrothermal fluids: evidence from quartz-epidote metasomatites of the Haldzan Buragtag massif, Mongolian Altai. Can. Mineral. 53, 1015–1034. https://doi.org/10.3749/canmin.1400023.
Macdonald, R., Bagiński, B., Zozulya, D., 2017. Differing responses of zircon, chevkinite-(Ce), monazite-(Ce) and fergusonite-(Y) to hydrothermal alteration: Evidence from the Keivy alkaline province, Kola Peninsula, Russia. Mineral. Petrol. 111, 523–545. https://doi.org/10.1007/s00710-017-0506-2.
Masau, M., Černý, P., Cooper, M.A., Chapman, R., Grice, J., 2002. Monazite-(Sm), a new member of the monazite group from the annie claim #3 granitic pegmatite, Southeastern Manitoba. Can. Mineral. 40, 1649–1655. https://doi.org/10.2113/gscanmin.40.6.1649.
Merlet, C., 1994. An accurate computer correction program for quantitative electron probe microanalysis. Microchim. Acta 114, 363–376. https://doi.org/10.1007/BF01244563.
McLennan, S.M., Taylor, S.R., 1979. Rare-earth element mobility associated with uranium mineralization. Nature 282, 247–250. https://doi.org/10.1038/282247a0.
Migdisov, A.A., Williams-Jones, A.E., Wagner, T., 2009. An experimental study of the solubility and speciation of the Rare Earth Elements (III) in fluoride- and chloride-bearing aqueous solutions at temperatures up to 300 degrees C. Geochim. Cosmochim. Acta 73, 7087–7109. https://doi.org/10.1016/j.gca.2009.08.023.
Mikhailova, J.A., Pakhomovsky, Ya.A., Ivanyuk, G.Yu., Bazai, A.V., Yakovenchuk, V.N., Elizarova, I.R., Kalashnikov A.O., 2017. REE mineralogy and geochemistry of the Western Keivy peralkaline granite massif, Kola Peninsula, Russia. Ore Geol. Rev. 82, 181–197. doi:10.1016/J.Oregeorev.2016.11.006.
Mills, S.J., Kartashov, P.M., Kampf, A.R., Konev, A.A., Koneva, A.A., Raudsepp, M., 2012. Cordylite-(La), a new mineral species in fenite from the Biraya Fe–REE deposit, Irkutsk, Russia. Can. Mineral. 50, 1281–1290.
Mineev, D.A., 1963. Geochemical differentiation of rare-earth elements. Geokhimiya 12, 1082–1100.
Mineev, D.A., 1968. Geochemistry of apogranites and rare-metal metasomatites of Northwestern Tarbagatai. Nauka, Moscow.
Mitrofanov, F.P., Zozulya, D.R., Bayanova, T.B., Levkovich, N.V., 2000. The world's oldest anorogenic alkali granitic magmatism in the Keivy structure on the Baltic Shield. Dokl. Earth Sci. 374, 1145–1148.
Möller, P., 1989. In: Lanthanides, Tantalum and Niobium. Springer, Berlin, Heidelberg, pp. 103–144. https://doi.org/10.1007/978-3-642-87262-4_4.
Nakada, R., Shibuya, T., Suzuki, K., Takahashi, Y., 2017. Europium anomaly variation under low-temperature water-rock interaction: a new thermometer. Geochem. Int. 55, 822–832. https://doi.org/10.1134/S001670291709004X.
Nilssen, B., 1970. Samarskites. Chemical composition, formula and crystalline phases produced by heating. Nor. Geol. Tidsskr. 50, 357–373.
Olivo, G.R., Williams-Jones, A.E., 1999. Hydrothermal REE-rich eudialyte from the Pilanesberg Complex, South Africa. Can. Mineral. 37, 653–663.
Pekov, I.V., Chukanov, N.V., Kononkova, N.N., Yakubovich, O.V., Massa, W., Voloshin, A.V., 2008. Tveitite-(Y) and rare-earth enriched fluorite from amazonite pegmatites of Western Keivy, Kola Peninsula, Russia. Genetic crystal-chemistry of natural Ca,REE-fluorides. Zapiski RMO 137, 76–93.
Pouchou, J.L., Pichoir, J.F., 1991. Quantitative analysis of homogeneous or stratified microvolumes applying the model 'PAP'. In: Newbury, H. (Ed.), Electron Probe Quantitation. Plenum Press, New York, pp. 31–75.
Prol-Ledesma, R.-M., Melgarejo, J.C., Martin, R.F., 2012. The El Muerto "NYF" granitic pegmatite, Oaxaca, Mexico, and its striking enrichment in allanite-(Ce) and monazite-(Ce). Can. Mineral. 50, 1055–1076.
Nishimori, R.K., Ragland, P.C., Rogers, J.J.W., Greenberg, J.K., 1977. Uranium deposits in granitic rocks, A report to the Energy Rsearch and Development Administration. University of North Carolina at Chapel Hill.
Roy, M., Dhana Raju, R., 1999. Petrogenetic model of A-type granitoids of the Kullampatti area, Salem District, Tamil Nadu, India. Gondwana Res. 2, 127–135. https://doi.org/10.1016/S1342-937X(05)70133-7.
Ruschel, K., Nasdala, L., Rhede, D., Wirth, R., Lengauer, C.L., Libowitzky, E., 2010. Chemical alteration patterns in metamict fergusonite. Eur. J. Mineral. 22, 425–433.
Salvi, S., Williams-Jones, A.E., 1996. The role of hydrothermal processes in concentrating

HFSE in the Strange Lake peralkaline complex, northeastern Canada. Geochim. Cosmochim. Acta 60, 1917–1932.
Salvi, S., Williams-Jones, A.E., 2005. Alkaline granite-syenite hosted deposits, in: Linnen, R.L., Samson, I.M., (Eds), Rare-Element Geochemistry and Mineral Deposits Short Course Notes, Geological Association of Canada Short Course Notes, 17, pp. 315–341.
Salvi, S., Williams-Jones, A.E., 2006. Alteration, HFSE mineralisation and hydrocarbon formation in peralkaline igneous systems: Insights from the Strange Lake Pluton, Canada. Lithos 91, 19–34.
Sami, M., Ntaflos, T., Farahat, E.S., Mohamed, H.A., Ahmed, A.F., Hauzenberger, C., 2017. Mineralogical, geochemical and Sr-Nd isotopes characteristics of fluorite-bearing granites in the Northern Arabian-Nubian Shield, Egypt: constraints on petrogenesis and evolution of their associated rare metal mineralization. Ore Geol. Rev. 88, 1–22.
Samson, I.M., Wood, S.A., 2005. The rare-earth elements: Behavior in hydrothermal fluids and concentration in hydrothermal mineral deposits, exclusive of alkaline settings, in: Linnen, R.L., Samson, I.M. (Eds), Rare-Element Geochemistry and Mineral Deposits, Geological Association of Canada Short Course Notes, 17, pp. 269–297.
Schmitt, A.K., Trumbull, R.B., Dulski, P., Emmermann, R., 2002. Zr-Nb-REE mineralization in peralkaline granites from the Amis Complex, Brandberg (Namibia): evidence for magmatic pre-enrichment from melt inclusions. Econ. Geol. 97, 399–413.
Sheard, E.R., Williams-Jones, A.E., Heiligmann, M., Pederson, C., Trueman, D.L., 2012. Controls of the concentration of zirconium, niobium, and the rarer earth elements in the Thor Lake rare metal deposit, Northwest Territories, Canada. Econ. Geol. 107, 81–104.
Simmons, W.B., Webber, K.L., 2008. Pegmatite genesis: state of the art. Eur J Mineral 20, 421–438.
Smith, M.P., Henderson, P., Campbell, L.S., 2000. Fractionation of the REE during hydrothermal processes: Constraints from the Bayan Obo Fe-REE-Nb deposit, Inner Mongolia, China. Geochim. Cosmochim. Acta 64, 3141–3160.
Sun, S.S., McDonough, W.F., 1989. Chemical and isotopic systematics of oceanic basalts: Implications for mantle composition and processes. Geol. Soc. Lond. Spec. Publ. 42, 313–345.
Taylor, R.P., Strong, D.F., Fryer, B.J., 1981. Volatile control of contrasting trace-element distributions in peralkaline granitic and volcanic-rocks. Contrib. Mineral. Petrol. 77, 267–271. https://doi.org/10.1007/bf00373542.
Tomašić, N., Gajović, A., Bermanec, V., Su, D.S., Rajić Linarić, M., Ntaflos, T., Schlögl, R., 2006. Recrystallization mechanisms of fergusonite from metamict mineral precursors. Phys. Chem. Minerals 33, 145–159. https://doi.org/10.1007/s00269-006-0061-6.
Trueman, D.L., Pedersen, J.C., de St Jorre, L., Smith, D.G.W., 1988. The Thor Lake rare-metal deposits, North-West Territories, in: Taylor, R.P., Strong, D.F. (Eds), Recent Advances in the Geology of Granite-Related Mineral Deposits, Canadian Institute of Mining and Metallurgy, 39, pp. 280–290.
Uher, P., Ondrejka, M., Konečny, P., 2009. Magmatic and post-magmatic Y-REE-Th phosphate, silicate and Nb-Ta-Y-REE oxide minerals in A-type metagranite: an example from the Turčok massif, the Western Carpathians, Slovakia. Mineral. Mag. 73, 1009–1025.
Voloshin, A.V., Lyalina, L.M., Savchenko, Ye.E., Bogdanova, A.N., 2003. Formanite-(Y) from the amazonite randpegmatites of Western Keivy (Kola Peninsula). Zapiski RMO 132, 82–93.
Voloshin, A.V., Pakhomovskii, Ya.A., 1986. Minerals and Evolution of Mineral Formation in Amazonite Pegmatites of the Kola Peninsula. Nauka, Leningrad.
Weilang, G., 1991. Chemistry and evolution of fergusonite-group minerals, Bayan Obo, Inner Mongolia. Chin. J. Geochem. 10, 266–276.
Williams-Jones, A.E., Samson, I.M., Olivo, G.R., 2000. The genesis of hydrothermal fluorite-REE deposits in the Gallinas Mountains, New Mexico. Econ. Geol. Bull. Soc. Econ. Geol. 95, 327–341. https://doi.org/10.2113/95.2.327.
Wood, S.A., 1990. The aqueous geochemistry of the rare earth elements and yttrium. Part II. Theoretical predictions of speciation in hydrothermal solutions to 350°C at saturated water vapor pressure. Chem. Geol. 88, 99–125.
Wood, S.A., 2005. The aqueous geochemistry of zirconium, hafnium, niobium and tantalum: in Linnen, R.L., Samson, I.M. (Eds), Rare-Element Geochemistry and Mineral Deposits, Geological Association of Canada Short Course Notes 17, pp. 217–268.
Wylie, A.W., 1954. Lanthanon and Scandium distribution in Western Australian Fergusonite. Am. Mineral. 39, 667–669.
Zozulya, D.R., Bayanova, T.B., Eby, G.N., 2005. Geology and age of the Late Archean Keivy alkaline province, Northeastern Baltic Shield. J. Geol. 113, 601–608. https://doi.org/10.1086/431912.
Zozulya, D.R., Kudryashov, N.M., Lyalina, L.M., Stepenshchikov, D.G., 2017. Late Archean rare-element pegmatites from Keivy-Kolmozero zone, Kola Peninsula, and dating (ID-TIMS, EMP) of pegmatitic zircon, microlite, monazite and thorite. In: Zaitsev, V.A., Ermolaeva, V.N. (Eds.), Magmatism of the Earth and related strategic metal deposits. GEOKHI RAS, Moscow, pp. 332–334.
Zozulya, D.R., Lyalina, L.M., Eby, N., Savchenko, Y.E., 2012. Ore geochemistry, zircon mineralogy, and genesis of the Sakharjok Y-Zr deposit, Kola Peninsula, Russia. Geol. Ore Deposits 54, 81–98. https://doi.org/10.1134/s1075701512020079.
Zozulya, D.R., Lyalina, L.M., Savchenko, Ye.E., 2015. Britholite ores of the Sakharjok Zr–Y–REE deposit, Kola Peninsula: geochemistry, mineralogy, and formation stages. Geochem. Int. 53, 892–902. https://doi.org/10.1134/S0016702915080108.
Zozulya, D., Lyalina, L., Macdonald, R., Bagiński, B., Savchenko, Y., Jokubauskas, P., 2019. Britholite group minerals from REE-rich lithologies of Keivy alkali granite—nepheline syenite complex, Kola Peninsula, NW Russia. Minerals 9, 732. https://doi.org/10.3390/min9120732.